UCSF
UC San Francisco Electronic Theses and Dissertations

Title
Role and circuit mechanism of cue-evoked neuronal inhibition in basolateral amygdala

Permalink
https://escholarship.org/uc/item/4c44r6v5

Author
Vitale, Kate

Publication Date
2015

Peer reviewed|Thesis/dissertation

eScholarship.org Powered by the California Digital Library
University of California

Role and circuit mechanism of cue-evoked neuronal inhibition in basolateral amygdala

by

Katherine Vitale

DISSERTATION

Submitted in partial satisfaction of the requirements for the degree of

DOCTOR OF PHILOSOPHY

in

Neuroscience

in the

GRADUATE DIVISION

of the

UNIVERSITY OF CALIFORNIA, SAN FRANCISCO

Copyright 2015 by

Katherine Vitale

All rights reserved

ACKNOWLEDGEMENTS

I dedicate this dissertation to my sister, Anna Vitale, who died in the last few weeks of its preparation. She and another sister, Liz Vitale, have dealt with schizophrenia for their entire adult lives, and their suffering is a main reason for my interest in neuroscience. I hope to contribute to helping individuals with mental illness during my lifetime, although I regret my work did not benefit Anna during hers. I am so grateful to Anna and Liz for being kind and supportive big sisters despite their own struggles.

I would also like to thank my other sisters Bianca and Vicky Ridler, and my brother, Ben Vitale, as well as their partners: Chris, Matt, and Anne. Like Anna and Liz, they have been my cheerleaders and role models, and I feel incredibly lucky to have had so many people to look up to and learn from. I cherish our adult relationships and know that we will always be there for one another, no matter what time zone we are in. Thank you for that and for the nieces and nephew you have brought into my life.

I would also like to thank my parents, Barb Dearborn and Bill Vitale. They have shown an exceptional amount of strength and resilience while raising a complicated, blended family of 6 children. They created a positive, loving environment while working long hours to support us and make a real difference in their communities. Our family had its ups and downs, but throughout, they showed us that they would *always* be there for us, no matter what life threw our way. That knowledge was immensely helpful during my Ph.D. research, and I am so grateful for them.

I am also extremely grateful to my boyfriend, Adam Gilgoff, who has brought so much adventure, fun and happiness into my life. I can never thank him enough for, quite frankly,

taking care of me in the last several weeks of my Ph.D. During these difficult times, he's been a rock and a soft place to fall all at once, and I feel very lucky to have him as a partner.

I also have so many friends to thank for supporting me throughout my Ph.D. Current and former labmates – Mike Gill, Catriona Miller, Hong Nie, Lacey Sahuque, Catherine Woods, Becca Reese, Irene Grossrubatcher, Mimi Zou, Anthony Mefford, George Luu, Peter Fong, Ryan Young, Irina Merzlyak-Russell, Ronald Keiflin, Susan Sangha, Ginny Long, Zack Chaddick, Zayra Millan, Ben Saunders, Jocelyn Richard, Fred Ambroggi, Jenny Mitchell, Elyssa Margolis, Maggie Waung, Annabelle Bergenfeld, Julie Meffre, Elizabeth Steinberg, Sarah Fischbach-Weiss, Joe Boivin, Joe Driscoll and Jocelyn Breton – thank you for helping to shape my ideas, helping me to develop skills, and being wonderful friends and colleagues. I also extend particular thanks to Ben Saunders, Fred Ambroggi and Liz Steinberg for being excellent collaborators and friends. I couldn't ask for better people to work with.

I also thank my smart and fun classmates, who I respect immensely, especially Sama Ahmed who helped me considerably with my thesis defense talk. Thanks also to my long-term roommates Jessica Woodard, Emma Nace and Mariko Miyakawa for their understanding and companionship for 6 years. Other friends – Robin Nobleman, Zoe Speed, Liz Holloway, Nicole Alcolado, Halley Roback, Anna Laurence, Emma Cameron, Georgia McNeil, Cecilia Newton, Maia McCarron, the Woodard family, Alex Stokes, Shanni Silberberg, Alayna Liptak and many more that I'm surely forgetting – you were all so supportive during my time at UCSF, and I am so grateful.

Thank you to my dissertation committee: Michael Brainard, Linda Wilbrecht, and Loren Frank. I appreciate the guidance you provided in shaping my project and the respect and compassion you showed me in meetings. I am especially grateful to Loren Frank for his help

after Tricia left for Baltimore. Loren met with me weekly (or even more often at times) to advise me and make sure I was on track, and this was invaluable for me to continue to progress at this time. I can't thank him enough.

Similarly, I will always feel indebted to Howard Fields for adopting me after Tricia's move. His generosity in this gesture made an enormous difference in my life, allowing me to stay in San Francisco to finish my degree. In addition, he and his lab provided an exceptionally warm and inclusive environment and significantly contributed to my scientific growth. Howard and his lab encouraged me to be precise in my hypotheses and careful in my interpretations – scientific skills that are commonly undervalued. I am very grateful to them for taking me in.

Finally, I would like to thank Tricia Janak. I can't imagine a better mentor for my time at UCSF. She provided the perfect combination of support and independence that helped me grow as a scientist and a person. I am not sure I would have stayed in science if I had not joined her lab, which I believe is common among several of her students. Her faith in us pushes us to be better. I am truly inspired by her grace and wisdom in the face of adversity, and will always look to her as a role model. I look forward to seeing how her lab and career continue to grow.

ABSTRACT

Basolateral amygdala (BLA) neurons are excited by conditioned cues after appetitive or aversive Pavlovian conditioning, and these neuronal excitations are considered to be a substrate for cue-outcome associative learning. However, an equal or greater number of BLA neurons can be inhibited by conditioned cues, and the role and mechanism of this inhibitory signal are not understood. Here we show that 77% of BLA neurons demonstrate long-lasting inhibition during a reward-predictive cue that is positively correlated with both learning and extinction of reward seeking. Optogenetic activation of BLA projection neurons during cue presentation impaired conditioned behavior, consistent with cue-evoked inhibition in BLA causally contributing to this behavior. Pharmacological inactivation of the orbitofrontal cortex (OFC) and optogenetic inactivation of OFC axon terminals in BLA also reduced conditioned behavior, with pharmacological inactivation of OFC additionally diminishing BLA cue-evoked inhibitions. Together, these data reveal a new role for BLA neuronal inhibitions in conditioned behavior, and suggest that this signal is mediated in part by OFC axon projections to BLA, which may activate local interneurons.

TABLE OF CONTENTS

Title page i

Copyright page ii

Acknowledgements iii

Abstract vi

Table of Contents vii

List of Tables viii

List of Figures ix

Chapter 1: Orbitofrontal cortex mediates inhibition within the basolateral amygdala to promote appetitive Pavlovian conditioning 1

- Introduction 1
- Results 3
- Discussion 25
- Methods 32

References 42

Library release statement 48

LIST OF TABLES

Table 1 – Baseline firing rates of all recorded BLA neurons in various sessions 19

LIST OF FIGURES

Figure 1 – CS-evoked inhibitions track expression of conditioned behavior during acquisition 5

Figure 2 – CS^+-evoked inhibitions emerge during acquisition on Day 1 7

Figure 3 – Sustained inhibitory signaling and conditioned behavior triggered by the CS^- increase in the first conditioning session 8

Figure 4 – BLA neurons both gain and lose CS^+-excitatory responding on Day 1 9

Figure 5 – The proportion of BLA neurons with CS^+-evoked excitation does not change across conditioning sessions 9

Figure 6 – CS^+-evoked sustained inhibitions decline in extinction 11

Figure 7 – CS^+-excited neurons in extinction 13

Figure 8 – Optogenetic activation of BLA neurons during the CS^+ impairs conditioned behavior 14

Figure 9 – Most putative interneurons in BLA are CS^+-excited 16

Figure 10 – Putative BLA interneurons with sustained CS^+-evoked excitations 17

Figure 11 – OFC activity is required for robust CS^+-evoked inhibitions and conditioned behavior 18

Figure 12 – Effect of OFC inactivation or saline infusion on CS^+-excited BLA neurons 20

Figure 13 – Optogenetic inhibiton of OFC-to-BLA axon terminals impairs conditioned behavior 22

Figure 14 – OFC viral expression and projections 23

CHAPTER 1

Orbitofrontal cortex mediates inhibition within the basolateral amygdala to promote appetitive Pavlovian conditioning

INTRODUCTION

How do animals learn which cues in their environment predict positive or negative outcomes? In mammals, a major site of plasticity underlying cue-outcome learning is the basolateral amygdala (BLA), which is composed of basal (BA) and lateral (LA) subnuclei. After learning that an auditory cue predicts a motivationally-significant outcome, such as footshock or sucrose, synaptic inputs onto LA from auditory thalamus are strengthened (McKernan and Shinnick-Gallagher, 1997; Tye et al., 2008) and activation of LA neurons in response to the cue is potentiated (Quirk et al., 1995; Tye et al., 2008). A common proposal is that this enhanced responding to the conditioned cue in LA is relayed to BA and subsequently to downstream regions to promote conditioned behavioral and physiological responding to the cue (Maren and Quirk, 2004; Pape and Pare, 2010; Janak and Tye, 2015).

Consistent with this notion, BLA neurons show cue-evoked increases in firing rate ("cue-excitation") after associative learning that correlate with behavioral expression of conditioning (Amano et al., 2011; Ambroggi et al., 2008; Herry et al., 2008; Muramoto et al., 1993; Paton et al., 2006; Sangha et al., 2013; Shabel and Janak, 2009; Tye and Janak, 2007; Tye et al., 2008). However, cue-evoked decreases in BLA neuronal firing rates ("cue-inhibition") have also been observed after learning (Amano et al., 2011; Ambroggi et al., 2008; Muramoto et al., 1993;

Sangha et al., 2013; Shabel and Janak, 2009; Tye et al., 2008), raising the question of the role and mechanism of this inhibitory signal.

Here we use electrophysiological, pharmacological and optogenetic approaches to examine the behavioral function of cue-evoked neuronal inhibitions in the BLA, and the dependence of these inhibitions on efferent projections. We focused on the dense, excitatory projection from orbitofrontal cortex (OFC) to BLA as a potential contributor because it shows neuronal encoding of outcome expectation or value during cue presentation (Belova et al., 2007; Paton et al., 2006; Schoenbaum et al., 1998, 1999), and lesions of the OFC impair such cue-outcome encoding within the BLA (Saddoris et al., 2005). We report that that 77% of BLA neurons demonstrate long-lasting inhibition during a reward-predictive cue that is positively correlated with both learning and extinction of reward seeking. In addition, optogenetic activation of BLA neurons during the conditioned cue impaired expression of conditioned behavior in well-trained rats. These findings are consistent with the hypothesis that cue-evoked inhibition in BLA causally contributes to conditioned responding to reward-predictive cues. Further, cue-evoked neuronal inhibitions in BLA were shown to depend on neural activity in the orbitofrontal cortex (OFC), and inactivation of the OFC or optogenetic inhibition of OFC axon terminals in BLA impaired conditioned behavior. Together, these findings highlight the contribution of BLA cue-evoked neuronal inhibitions in cue-elicited reward-seeking behavior and identify a new role for the OFC in contributing to both cue-evoked BLA inhibitions and cue-driven behavioral responding.

RESULTS

Cue-evoked inhibition in BLA emerges during acquisition and is correlated with expression of conditioned behavior

If cue-evoked inhibition drives conditioned behavioral responding, it should emerge during acquisition of conditioning. To test this, we recorded BLA single units in rats (n=18) over 7 daily sessions as they learned a cue-reward conditioned association (Figures 1A and 1B). We predicted that BLA inhibition time-locked to the reward-predictive cue would develop during acquisition. In the conditioning procedure, a 30-s auditory stimulus (CS^+) was repeatedly paired with sucrose delivery, whereas a different 30-s stimulus (CS^-) was paired with nothing. Sucrose delivery occurred once during each CS^+ beginning at a variable latency after cue onset. Usually this latency ranged between 10-24 s, but on ~6% of trials, it was 1 s. Trials with 1-s reward latency were included to maintain behavioral responding during the first 10 s of the CS^+, but were omitted from the final analysis such that this 10-s window after cue onset could be used to analyze conditioned neural and behavioral responses. Behavioral measures of conditioning included percent time spent in the sucrose delivery port during this 10-s period and latency to enter the port after CS onset.

Behavioral responding to the CS^+ and CS^- changed differentially across the seven conditioning sessions, as indicated by a significant interaction between cue type and session in two-way repeated measures ANOVA analyses for both percent time in port ($F_{4.034,68.580}$=59.959, $p<10^{-21}$) and port entry latency ($F_{6,102}$=82.996, $p<10^{-36}$). Across sessions, rats increased the amount of time they spent in the port during the CS^+ and reduced their latency to enter the port during this cue (Figures 1C and 1D; time in port: main effect of session, $F_{6,102}$=39.398, $p<10^{-23}$, Day 1 vs. Day 7, $p<10^{-8}$, Bonferroni-corrected post-hoc comparison; latency: main effect of

session: $F_{2.721,46.263}$=40.768, $p<10^{-11}$, Day 1 vs. Day 7: $p<10^{-6}$). Conversely, conditioned behavior in response to the CS^- decreased across training sessions, likely due to initial generalization of conditioned behavior to the CS^- in session 1, followed by cue discrimination in subsequent sessions (Figures 1C and 1D; decrease in time in port, main effect of session: $F_{3.138,53.352}$=7.486, $p<0.001$, Day 1 vs. Day 7: $p<0.05$; increase in latency: main effect of session: $F_{3.470,58.996}$=15.378, $p<10^{-7}$, Day 1 vs. Day 7: $p<0.01$).

Mirroring these behavioral changes, the proportion of BLA neurons with inhibitory responses triggered by the CS^+ more than tripled across conditioning sessions from 24.8% (31/125) on Day 1 to 76.6% (108/141) on Day 7 (Figures 1E and 1F; χ^2=71.249, $p<10^{-16}$). Inhibitions began at a short latency after CS^+ onset and were long-lasting, persisting throughout the 10-s cue analysis period (Figure 1G). This short latency indicates that cue presentation and not port entry behavioral responding triggered inhibitions, since the latter occurred at an average latency of ~5 s in trained animals (Figure 1D).

Conversely, the proportion of neurons with sustained inhibitions during the CS^- significantly decreased from 17.600% (22/125) on Day 1 to 9.220% (13/141) on Day 7 (Figures 1E and 1H; χ^2=4.07, $p<0.05$), reflecting the decrease in conditioned behavior during the CS^- across training sessions. Thus, during acquisition of conditioning, the size of the population of neurons inhibited by a given cue reflects the strength of expression of conditioned behavior in response to that cue.

Given this evidence that sustained CS^+-evoked inhibitions increase across conditioning sessions, we investigated whether they begin to emerge on the first day of training, Day 1. Subjects showed evidence of learning across trials on Day 1. The percent time spent in the sucrose port during the first 10 s of the CS^+ increased over trials (Figure 2A; positive correlation

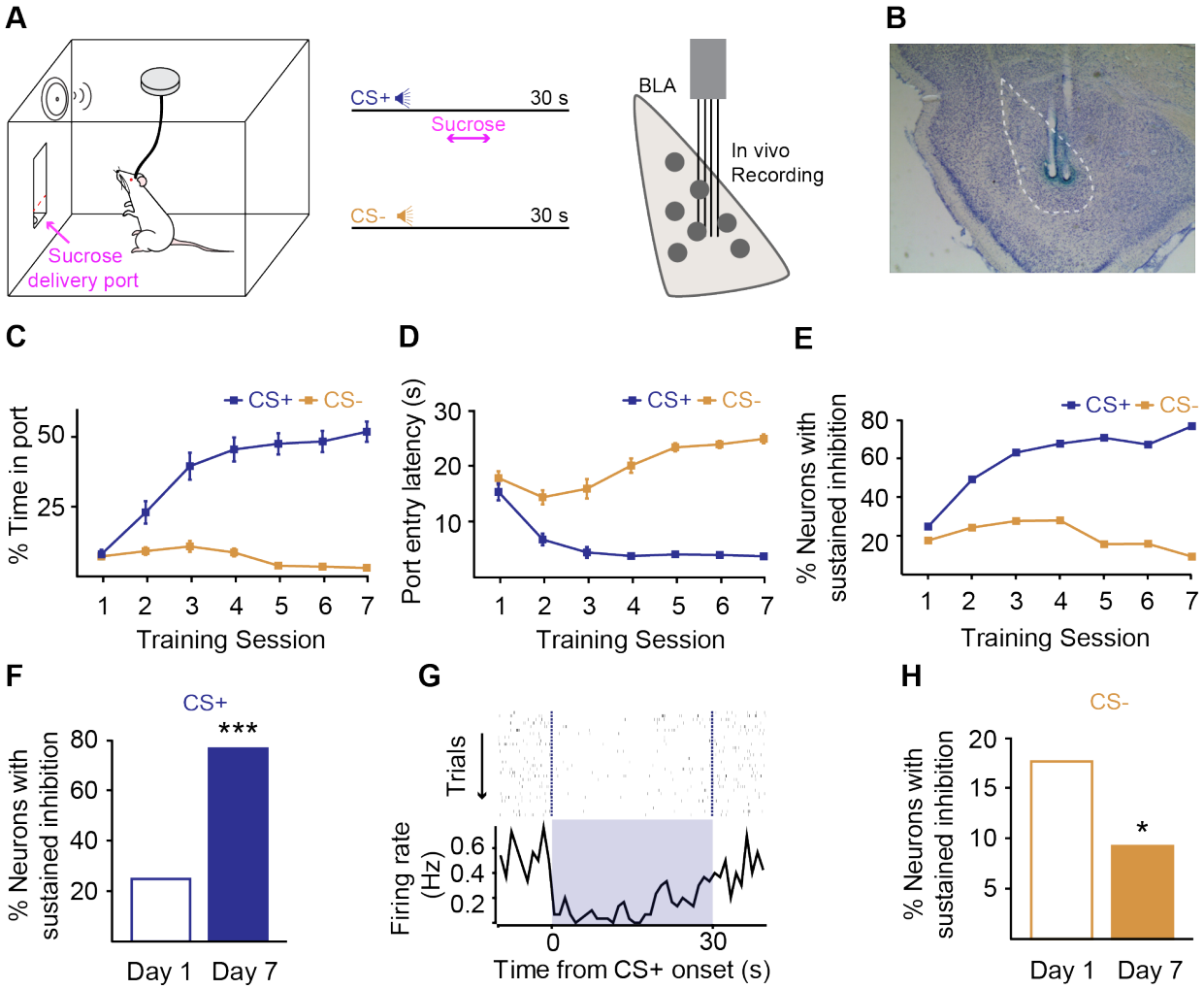

Figure 1: CS-evoked inhibitions track expression of conditioned behavior during acquisition
(A) Conditioning procedure: rats implanted with bilateral, single-wire, fixed electrode arrays in BLA were trained for 7 days on a Pavlovian conditioning task in which one 30-s auditory cue (CS+, either tone or white noise) was paired with sucrose delivery at a variable latency after CS+ onset (range: 1 s, 10-24 s), and the other cue (CS-) was paired with nothing. CS+ trials with 1-s sucrose delivery latency were excluded from all analyses.
(B) Example histology from a rat with electrode arrays in bilateral BLA.
(C) Percent time in the sucrose port during the first 10 s of the CS+ and CS- across training sessions (mean ± SEM). Time in port during the CS+ increased across sessions ($P<10^{-23}$, one-way ANOVA) and time in port during the CS- decreased ($P<10^{-8}$).
(D) Data are presented as in C, but for latency to enter the sucrose port after CS onset. Latency decreased across sessions for the CS+ ($P<0.001$) and increased across sessions for the CS- ($P<0.01$).
(E) Percentage of neurons with sustained inhibitions across training sessions for the CS+ and CS-.
(F) The percentage of neurons with sustained inhibitions triggered by the CS+ on Day 1 and Day 7. This measure is increased on Day 7 relative to Day 1 (***$P<10^{-16}$, chi-squared test).
(G) Peri-event raster and histogram aligned to CS+ onset from a representative BLA neuron recorded from a trained rat performing the conditioning task on Day 7. Trial number increases from top to bottom. Indigo squares in the raster indicate time of CS+ onset and offset on each trial and indigo shaded area on the histogram spans the period of the CS+. Histogram bin size is 1 s.
(H) Data are presented as in F, but for the CS-. The percentage of neurons with sustained inhibitions during the CS- significantly decreased between sessions (Day 1 vs. Day 7, *$P<0.05$, chi-squared test).

with trial number; R^2= 0.041, $p<10^{-4}$), while the latency to enter the port after CS^+ onset decreased over trials (Figure 2B; negative correlation with trial number; R^2= 0.130, $p<10^{-14}$). In addition, we observed BLA neurons that developed sustained inhibitions during the CS^+ on Day 1 (Figure 2C). To quantify the development of sustained inhibitions in the entire population of BLA neurons recorded on Day 1 (N=125, 16 rats), we performed a regression analysis to determine how the mean z-scored firing rate in the first 10 s of the CS^+ of this population changed across trials of the first training session. We found there was a significant negative correlation of mean normalized CS^+-evoked neuronal response with trial number (Figure 2D, R^2=0.012, $p<10^{-9}$), suggesting that sustained inhibitory responding during the CS^+ increased during the session. Again, this increase in inhibition is unlikely to be driven by the port entry behavior per se since the correlation remains when only the first 500 ms of neural activity after CS^+ onset is analyzed (Figure 2E; R^2= 0.01, $p<10^{-8}$), a time period with few port entry responses. In addition, significantly more neurons increased (18/125, 14.4%) rather than decreased (5/125, 4%) sustained inhibitory CS^+ responding (χ^2=8.09, p<0.01). Notably, rats that acquired conditioned behavior quickly on Day 1, as indicated by a shorter mean port entry latency in response to the CS^+, tended to have more neurons with sustained CS^+-evoked inhibitions on Day 1 (Figure 2F; R^2 = 0.302, p<0.05). Taken together, these findings suggest that acquisition of conditioned behavior is correlated with emergence of sustained cue-evoked inhibition.

The magnitude of sustained neural inhibition in response to the unrewarded CS^- also increased across trials on Day 1 (Figure 3A; correlation with trial number: R^2= 0.003, p<0.01). This likely reflects generalization of behavioral responding to the CS^- as port entry behavior in response to the CS^- also increased in the first session (Figures 3B and 3C; time in port correlation with trial number: R^2=0.01, p<0.05, port entry latency correlation with trial number:

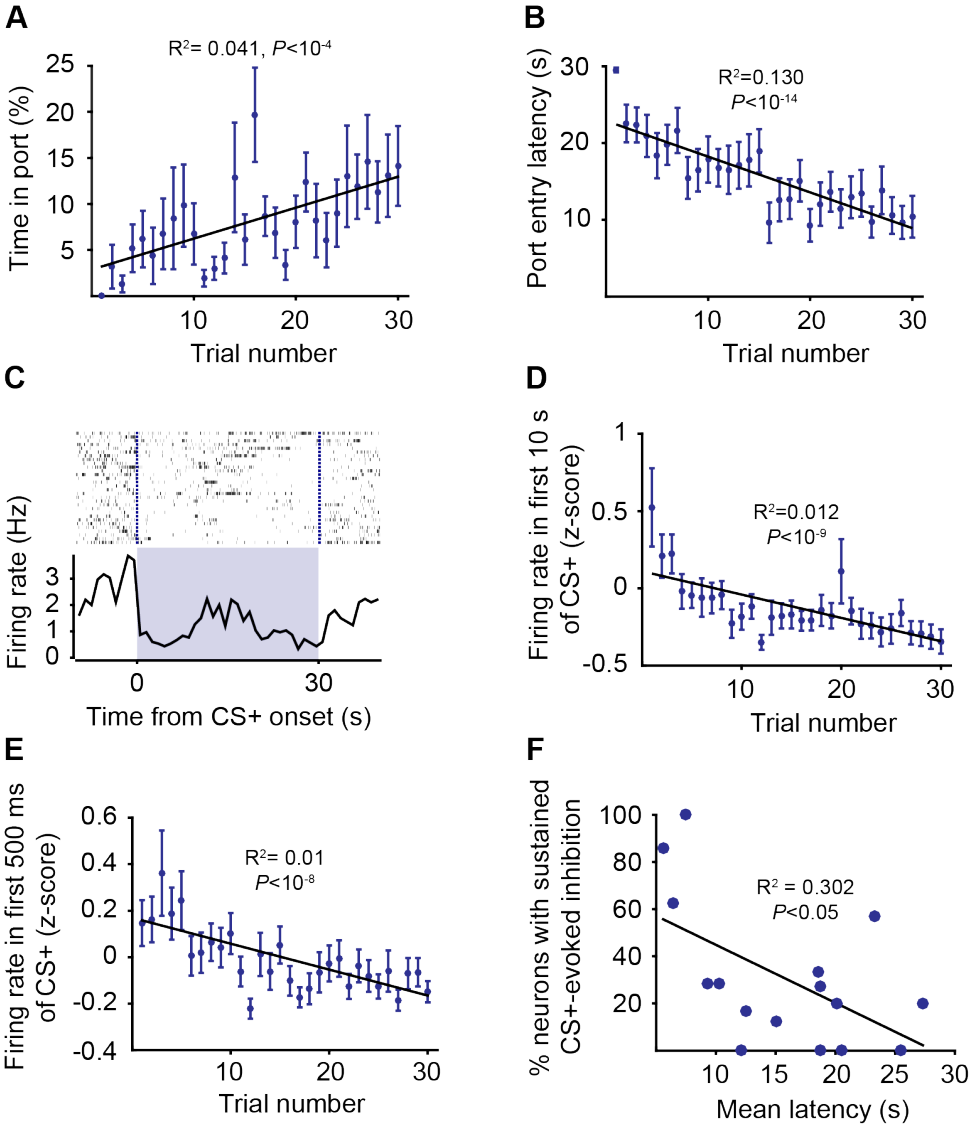

Figure 2: CS+-evoked inhibitions emerge during acquisition on Day 1
(A) Percent time in the port during the first 10 s of the CS+ (mean ± SEM) across trials of the Day 1 conditioning session. Percent time in port of all rats positively correlated with trial number (R^2= 0.041, $P<10^{-4}$).
(B) Data presented as in A, but for latency. Latency of all rats negatively correlated with trial number (R^2=0.130, $P<10^{-14}$).
(C) Peri-event raster and histogram aligned to CS+ onset from a BLA neuron that developed a sustained inhibition triggered by the CS+ on Day 1.
(D) Normalized firing rate during the first 10 s of the CS+ of all BLA neurons recorded on Day 1 (mean ± SEM) across trials. Firing rates were z-scored using a 10-s pre-CS+ baseline period. This measure negatively correlated with trial number (R^2=0.012, $P<10^{-9}$).
(E) Data presented as in D, but for normalized firing rate during the first 500 ms of the CS+. Baseline firing rate was calculated as the average of all 500 ms bins during the 10 s pre-CS+ period. This measure negatively correlated with trial number (R^2= 0.01, $P<10^{-8}$).
(F) Rats' mean port entry latency on Day 1 plotted in relation to the proportion of rats' BLA neurons with sustained inhibitions. Negative correlation: R^2 = 0.302, $P<0.05$.

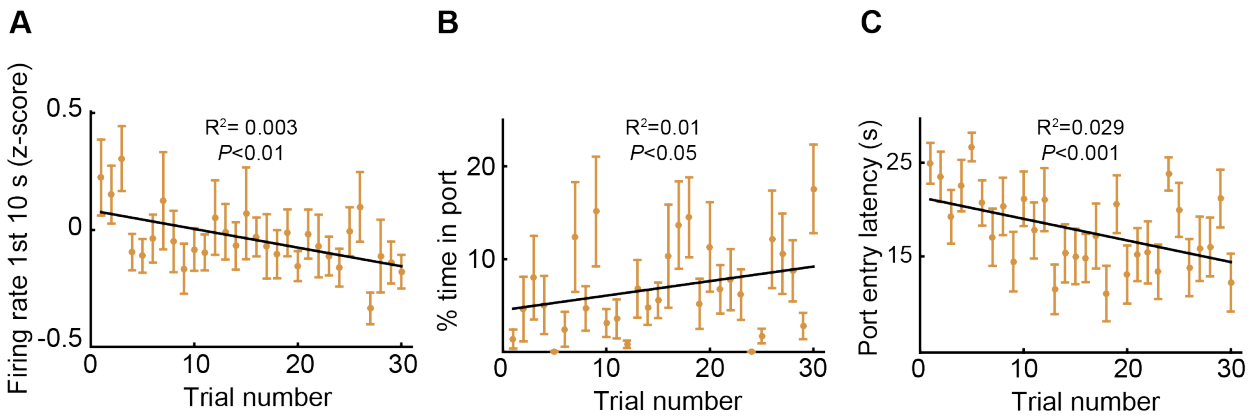

Figure 3: Sustained inhibitory signaling and conditioned behavior triggered by the CS- increase in the first conditioning session
(A) Normalized firing rate of all recorded BLA neurons during the first 10 s of the CS- (mean ± SEM) across trials of the Day 1 conditioning session. There was a negative correlation between normalized firing rate and trial number (R^2= 0.003, *P*<0.01).
(B) Percent time in port during the first 10 s of the CS- (mean ± SEM) across trials of the conditioning session on Day 1. There was a positive correlation between percent time in port and trial number (R^2=0.01, *P*<0.05).
(C) Port entry latency after CS- onset (mean ± SEM) across trials of the first conditioning session. There was a negative correlation between latency and trial number (R^2=0.029, *P*<0.001).

R^2=0.029, p<0.001). Therefore, increases in both CS^+- and CS^--evoked inhibition on Day 1 track the increases in behavioral responding to these cues, supporting the hypothesis that inhibitory BLA signaling promotes conditioned cue responding.

Interestingly, the mean normalized population response of BLA neurons begins significantly above zero and becomes negative over the course of the session (Figure 2D and 2E), this could suggest neurons were both losing CS^+-evoked excitation and gaining CS^+-evoked inhibition. Indeed, we found that more neurons decreased rather than increased excitatory responding (15/125= 12% decreased versus 4/125 = 3.2% increased, χ^2=6.892, p<0.01). Perhaps because rats were not habituated to the auditory stimuli prior to conditioning sessions, this subset of BLA neurons initially may have demonstrated novelty-related activation in response to the CS^+ that diminished in subsequent trials (Figure 4A). Neurons that increased excitatory

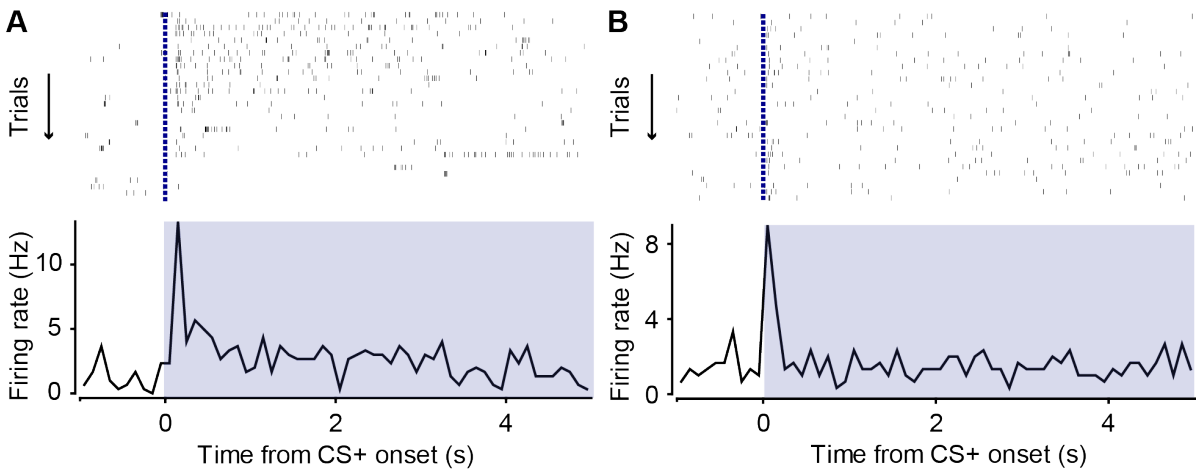

Figure 4: BLA neurons both gain and lose CS+-excitatory responding on Day 1
(A) Peri-event raster and histogram of a neuron that loses CS+-evoked excitation across trials of Day 1. Bin size: 100 ms.
(B) Peri-event raster and histogram of a neuron that gains CS+-excitatory responding across trials of Day 1. Bin size: 100 ms.

responding throughout the session (Figure 4B) are consistent with the established role of cue-excited neurons in promoting conditioned behavior (Ambroggi et al., 2008; Herry et al., 2008, Tye et al., 2008). In addition, there was no change in the proportion of BLA neurons excited by the CS^+ between Day 1 (22.4%, 28/125) to Day 7 (19.1%, 27/141) (Figures 5A and 5B; χ^2=0.43, p=0.514). We speculated this reflected loss of CS^+-evoked excitation during habituation on Day 1, as well as development of a population of excitatory neurons encoding appetitive auditory conditioned cues in subsequent training sessions, as we have shown previously (Tye et al., 2008).

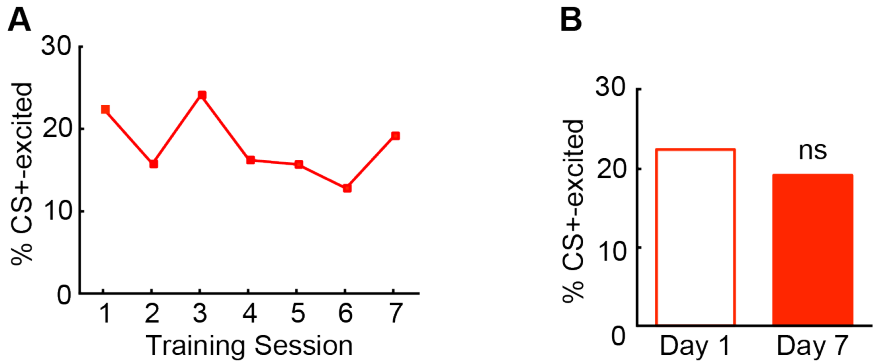

Figure 5: The proportion of BLA neurons with CS+-evoked excitation does not change across conditioning sessions
(A) Proportion of CS+-excited neurons in conditioning sessions 1-7.
(B) Proportion of CS+-excited neurons in conditioning sessions on Day 1 and Day 7. There was no significant change in the proportion between days.

Cue-evoked inhibition in BLA declines in extinction

Cue-evoked inhibition of BLA neurons should decrease during extinction if it contributes to behavioral responding to the CS^+. On Day 7, 14 rats underwent behavioral extinction immediately after the 7th conditioning session. During the extinction session, the CS^+ and CS^- were delivered as usual, but sucrose reward was omitted. On Day 8, recall of extinction memory was tested (Figure 6A).

As expected, conditioned behavior declined during the Day 7 extinction session as revealed by a negative correlation between percent time in port during the CS^+ and trial number (Figure 6B; R^2=0.174, $p<10^{-17}$), and a positive correlation between port entry latency after CS^+ onset and trial number (Figure 6C; R^2=0.2918, $p<10^{-30}$). The mean normalized CS^+ response of units identified on the Day 7 conditioning session as having a CS^+-evoked sustained inhibition significantly decreased across trials in extinction, but only when the entire first 10 s the CS^+ was analyzed (positive correlation of z-score with trial number: R^2= 0.0146, $p<10^{-9}$; Figure 6D); analysis of the normalized response in the first 500 ms of the CS^+ found no change over extinction trials (Figure 6E; R^2= 1.0928×10^{-5}, p=0.8633) indicating that a brief response at the onset of the CS+ remained.

These changes in behavioral and neuronal responding were maintained until the extinction recall session on Day 8. As compared to the final Day 7 conditioning session, the percent time in port during the CS^+ was decreased and port entry latency after the CS^+ was increased during extinction recall (Figures 6F and 6G; percent time in port: $p<10^{-3}$, Wilcoxon signed-rank test, port entry latency: $p<10^{-3}$, Wilcoxon signed-rank test). Further, there was a dramatic reduction in the number of neurons with sustained inhibitions during the CS^+ from 76.6% (108/141) on Day 7 before extinction to 34.1% (42/123) in the extinction recall session

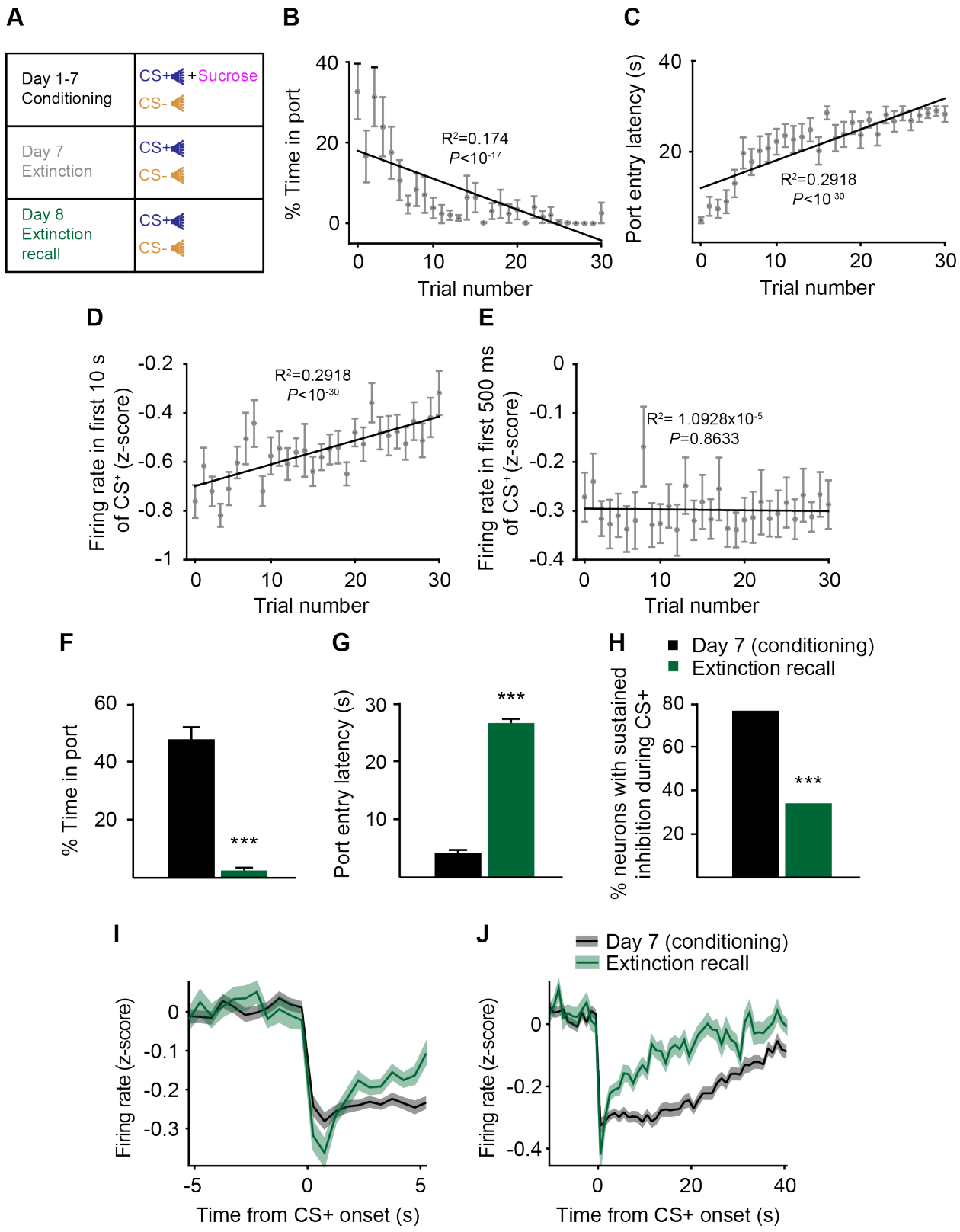
A
Day 1-7 Conditioning
CS+ +Sucrose
CS-
Day 7 Extinction
CS+
CS-
Day 8 Extinction recall
CS+
CS-
B
% Time in port
R²=0.174
P<10⁻¹⁷
Trial number
C
Port entry latency (s)
R²=0.2918
P<10⁻³⁰
Trial number
D
Firing rate in first 10 s of CS⁺ (z-score)
R²=0.2918
P<10⁻³⁰
Trial number
E
Firing rate in first 500 ms of CS⁺ (z-score)
R²= 1.0928x10⁻⁵
P=0.8633
Trial number
F
% Time in port
***
G
Port entry latency (s)
***
H
Day 7 (conditioning)
Extinction recall
% neurons with sustained inhibition during CS+
***
I
Firing rate (z-score)
Time from CS+ onset (s)
J
Day 7 (conditioning)
Extinction recall
Firing rate (z-score)
Time from CS+ onset (s)

Figure 6: ***(continued from previous page)*** **CS+-evoked sustained inhibitions decline in extinction**
(A) Extinction procedure: immediately after the last conditioning session on Day 7, rats underwent an extinction session that was identical to a regular conditioning session, except sucrose delivery was withheld. This approach allowed BLA neurons with sustained inhibitions identified during the Day 7 conditioning session to be tracked in extinction. On Day 8, a second extinction session served to assess neural activity during recall of extinction memory.
(B) Percent time in port during the CS+ (mean ± SEM) during trials of the extinction session on Day 7. There was a negative correlation between percent time in port for all rats and trial number (R^2=0.174, $P<10^{-17}$).
(C) Data are presented as in B, but for port entry latency. There was a positive correlation between latency for all rats and trial number (R^2=0.2918, $P<10^{-30}$).
(D) Normalized firing rate during the first 10 s of the CS+ of all BLA neurons with a sustained inhibition in the Day 7 conditioning session (mean ± SEM) measured on trials of the Day 7 extinction session. There was a positive correlation between this measure and trial number (R^2= 0.0146, $P<10^{-9}$).
(E) Data are presented as in D, but for normalized firing rate during the first 500 ms of the CS+ of all BLA neurons with a sustained inhibition during the Day 7 conditioning session. There was no correlation between this measure and trial number (R^2= 1.0928×10^{-5}, P=0.8633).
(F) Percent time in port during the first 10 s of the CS+ (mean ± SEM) in the Day 7 conditioning session and the Day 8 extinction recall session. Percent time in port was decreased in the extinction recall session compared to the Day 7 conditioning session (***$P<10^{-3}$, Wilcoxon signed-rank test).
(G) Data are presented as in F, but for port entry latency. Latency was increased in the extinction recall session compared to the Day 7 conditioning session (***$P<10^{-3}$).
(H) Percentage of neurons with sustained inhibition during the CS+ in the last conditioning session (Day 7) and the extinction recall session (Day 8). There was a large reduction in this percentage from 76.596% (108/141) on Day 7 before extinction to 34.146% (42/123) in the extinction recall session (***$P<10^{-11}$, chi-squared test).

(Figure 3H; χ^2=48.248, $p<10^{-11}$). As can be seen in the population response graphs (Figures 6I and 6J), in those neurons that retained a statistically significant CS^+-evoked inhibition in the extinction recall session, the decrease in firing rate is of shorter duration, similar to what we observed by the end of the initial extinction session. These findings suggest that the early-onset cue-evoked inhibition may represent savings of the original memory trace encoding the CS^+-US association, while the longer sustained inhibitory response may be related to ongoing behavior.

For neurons that were CS^+-excited in the final conditioning session, sustained excitatory CS^+ responses also declined during extinction (negative correlation with trial number: R^2=0.073, $p<10^{-8}$, Figure 7A), however there was no change in the normalized early response of this population (Figure 7B; R^2=2.50 x 10^{-4}, p=0.699). In addition, there was no change in the number of neurons excited by the CS^+ in the last training session (Day 7, 27/141, 19.1%) compared to the extinction recall session (Day 8, 23/123, 18.7%) (Figure 7C; χ^2=0.0087, p=0.9259). Because

excitatory CS^+ responding declined in extinction, the units recorded on the last conditioning session and the extinction recall session may be different, and these findings may be consistent with reports of distinct sets of neurons in BLA being activated by a conditioned cue after learning and after extinction (Amano et al., 2011; Herry et al., 2008).

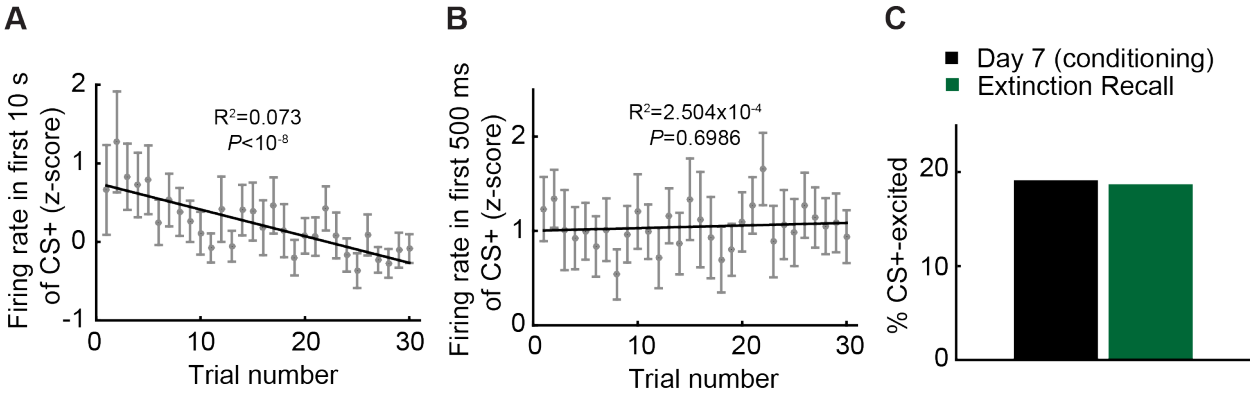

Figure 7: CS+-excited neurons in extinction
(A) Normalized firing rate in the first 10 s of CS+-excited neurons identified in the Day 7 conditioning session (mean ± SEM) across trials of the Day 7 extinction session. There wass a negative correlation between firing rate for all neurons and trial number (R^2=0.073, $P<10^{-8}$).
(B) Normalized firing rate in the first 500 ms of CS+-excited neurons identified in the Day 7 conditioning session (mean ± SEM) across trials of the Day 7 extinction session. There was no correlation between firing rate in this period for all neurons and trial number (R^2=2.504x10^{-4}, P=0.6986).
(C) The proportion of neurons with CS+-evoked excitation on the last conditioning session on Day 7, and the extinction recall session. There is no change in this proportion across sessions (χ^2=0.0087, P=0.9259).

Optogenetic activation of BLA neurons during the CS^+ reduces conditioned behavioral responding

If CS^+-evoked inhibitions in BLA neurons contribute to behavioral responding to the CS^+, then brief activation of BLA neurons during the CS^+ should serve to counter this inhibition and reduce behavioral responding. To test this hypothesis we expressed the light-sensitive cation channel ChR2 in BLA neurons, to allow their photoactivation through optical fibers implanted directly above the BLA (Figures 8A and 8B). After 7 sessions of training without light delivery,

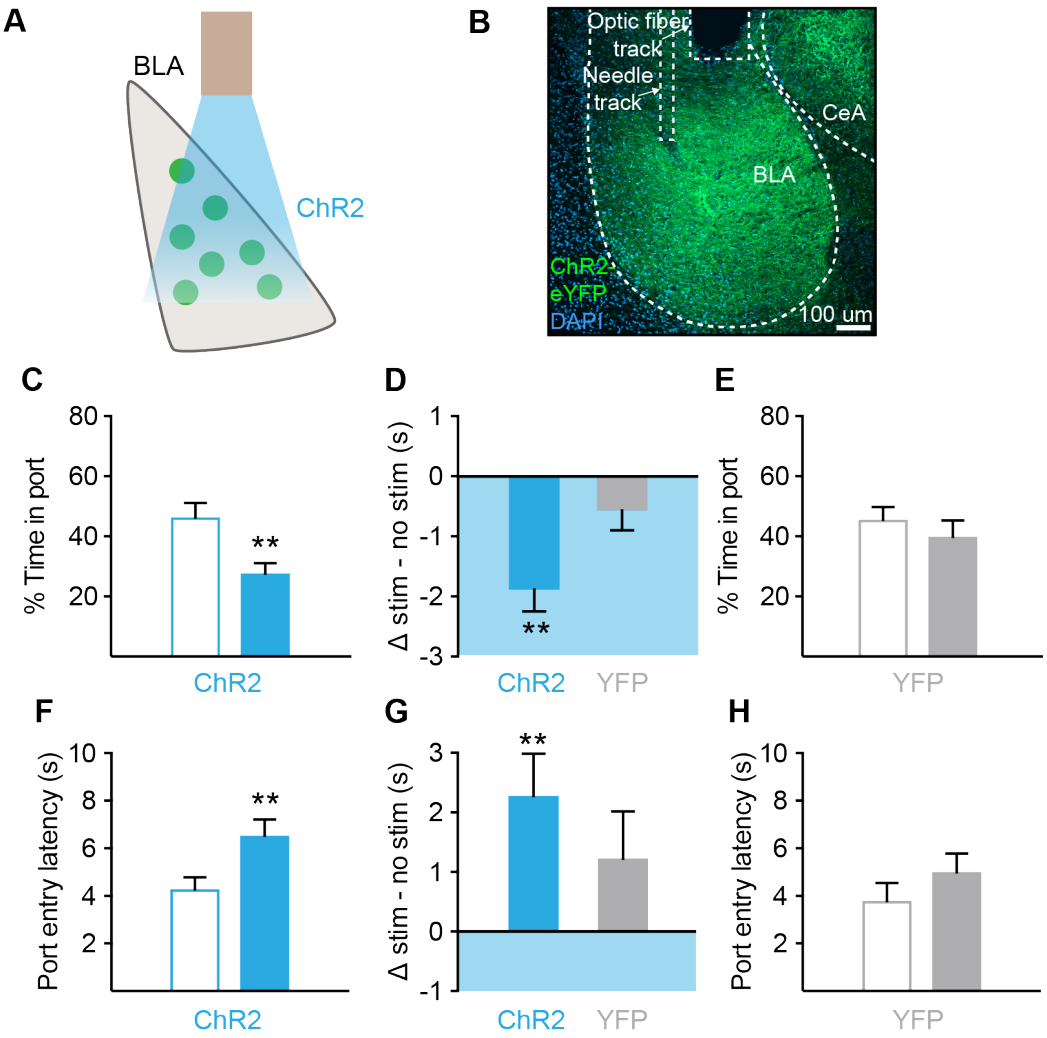

Figure 8: Optogenetic activation of BLA neurons during the CS+ impairs conditioned behavior

(A) Experimental approach for optogenetic activation experiment. Rats expressing AAV5-CaMKII-ChR2-YFP (n=9) or AAV5-CaMKII-YFP (n=6) in bilateral BLA and with optical fibers implanted above the site of infection were trained on the appetitive task described in Figure 1. On Day 8, light stimulation was paired with half of CS+ and CS- trials.

(B) Example histology of a rat showing virus infection and optical fiber placement in BLA.

(C) Percent time in port in the first 10 s of the CS+ during trials with (solid) and without (hollow) light stimulation (mean ± SEM). This measure was decreased during trials with stimulation compared to those without (**P<0.01).

(D) Difference in percent time in port between trials with and without stimulation (mean ± SEM) for ChR2-expressing rats and YFP-only controls. This measure was significantly different from zero for ChR2-expressing rats (**P<0.01), but not controls.

(E) Percent time in port in the first 10 s of the CS+ during trials with (solid) and without (hollow) light stimulation for YFP-only control rats. There was no significant difference in percent time in port for trials with and without stimulation for these rats (P=0.2188).

(F-H) Data are presented as in C-E, but for port entry latency. Latency was significantly decreased on stimulation trials compared to no stimulation trials for ChR2-expressing rats (**P<0.01), but not YFP-only controls (P=0.2188). The difference in latency between stimulation trials and no stimulation trials was significantly different than zero for ChR2-expressing rats (**P<0.01), but not YFP-only controls.

half of CS^+ trials were paired with light on Day 8. In this session, responding to the CS^+ was significantly reduced on trials in which light was delivered compared to no-light trials for ChR2 rats (p=0.0039; Figure 4C), and this change in time in port was significantly different from zero (one-sample test, p=0.0039; Figure 4D). Time spent in the port during the CS^+ was not affected by light delivery in control rats that expressed YFP-only virus (p=0.2188; Figure 4E). ChR2 rats were also slower to make a port entry on CS^+ light-on trials, compared to CS^+ no-light trials (p=0.0039; Figure 4F), a change that was significantly different from zero (one-sample test, p=0.0039, Figure 4G). There was no effect on port entry latency for YFP-only rats (p=0.2188; Figure 4H). These data are consistent with the hypothesis that BLA neuronal cue-evoked inhibition promotes conditioned behavioral responding.

Most putative inhibitory interneurons in BLA are activated by the CS^+

We next considered how BLA neuronal inhibitory responding to the CS^+ was generated. We hypothesized that local BLA interneurons (INs) could contribute to this signal by providing feed-forward inhibition onto other BLA neurons. We therefore predicted that we would see activation of putative BLA interneurons in response to the CS^+ in trained animals (Day 7 recording session). As reported previously (Courtin et al., 2014), putative INs form a distinct cluster in 3D space defined by spiking characteristics: log transformed baseline firing rate, the area under the after-hyperpolarization peak, and spike half-width (Figure 9A). We found that 9/13 (69%) of putative INs were excited by the CS^+, while this response was only seen in 9/128 (7%) of other BLA neurons (Figure 9B). In contrast, the vast majority of other neurons (98/128, 77%) and only 1/13 (7.7%) of putative INs demonstrated CS^+-evoked sustained inhibitions (Figure 5B). In addition, there was a significant difference between normalized responding in both the first 500

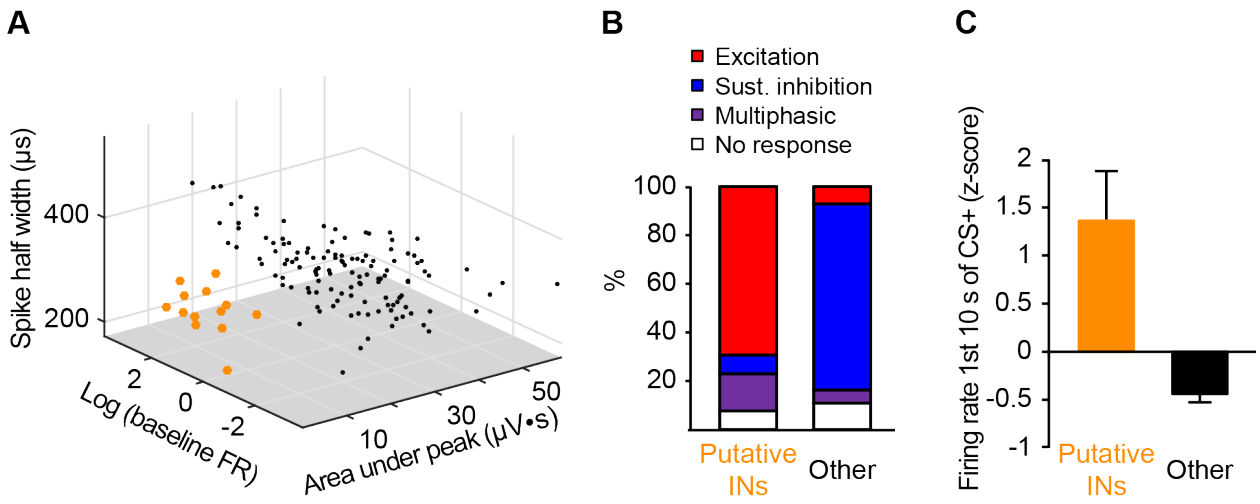

Figure 9: Most putative interneurons in BLA are CS+-excited
(A) All BLA neurons recorded on the last conditioning session on Day 7 were plotted in a 3D space defined by action potential half-width, baseline firing rate (log-transformed), and the area under the afterhyperpolarization peak. Putative interneurons (orange) were identified using a clustering algorithm, followed by manual delineation of a more restrictive cluster based on visual separation.
(B) Distribution of CS+-evoked responses in putative interneurons recorded on Day 7 and unidentified neurons. Multiphasic responses consisted of a brief excitation followed by a sustained inhibition.
(C) Normalized firing rate (mean ± SEM) of putative interneurons and other BLA neurons recorded on Day 7 in the first 10 s of the CS+. Putative interneurons have a higher firing rate during this period

ms and the first 10s of putative INs versus other neurons (Figure 5C). Indeed, a higher baseline firing rate correlated with a more positive z-score CS^+ response in both the early (R^2= 0.2545, $p<10^{-9}$) and sustained (R^2= 0.0472, $p<0.01$) response windows. In addition, excitatory responding by putative interneurons was sustained for a long period during the cue in 6/9 (66.667%) CS^+-excited putative interneurons, similar to inhibitory responding by other BLA neurons (Figure 10). These data are consistent with a model whereby BLA interneurons are activated during the CS^+ leading to feed-forward inhibition of other BLA neurons.

BLA inhibition and conditioned behavior are dependent on OFC activity

OFC sends excitatory projections to BLA (Aggleton et al., 1980; Amaral and Insausti, 1992) and has been shown to directly excite parvalbumin-expressing interneurons and glutamatergic projection neurons in the BLA complex (Smith et al., 2000). Furthermore, OFC

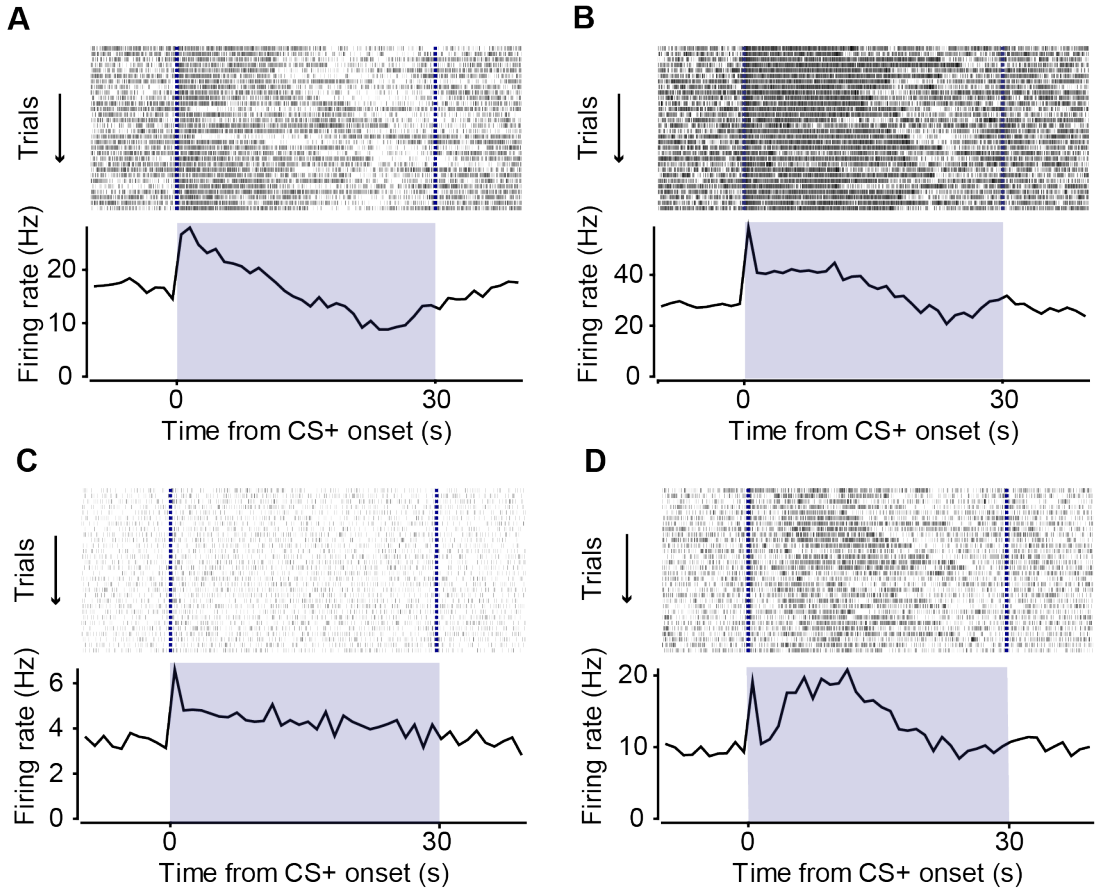

Figure 10: Putative BLA interneurons with sustained CS+-evoked excitations
(A-F): Peri-event rasters and histograms of 4 of the 6 putative interneurons with sustained CS+-evoked excitation on Day 7.

is proposed to encode expected outcome during reward-predictive cues and convey this signal to BLA (Schoenbaum et al., 1998, 1999, 2011). Therefore, we hypothesized that the OFC could be involved in cue-evoked activation of local BLA interneurons that subsequently suppress BLA projection neurons. If this is the case, suppression of neural activity in the OFC should decrease BLA cue-evoked inhibitions and thereby also decrease task performance (Figures 6A and 6B).

OFC inactivation, achieved via intra-OFC infusion of the GABA agonists, muscimol and baclofen (M/B), significantly attenuated CS^+-evoked inhibition in BLA neurons recorded in trained animals. Figure 11B shows an example of a neuron with a clear inhibitory response before OFC inactivation that is greatly diminished after M/B infusion. In addition, the mean CS^+-

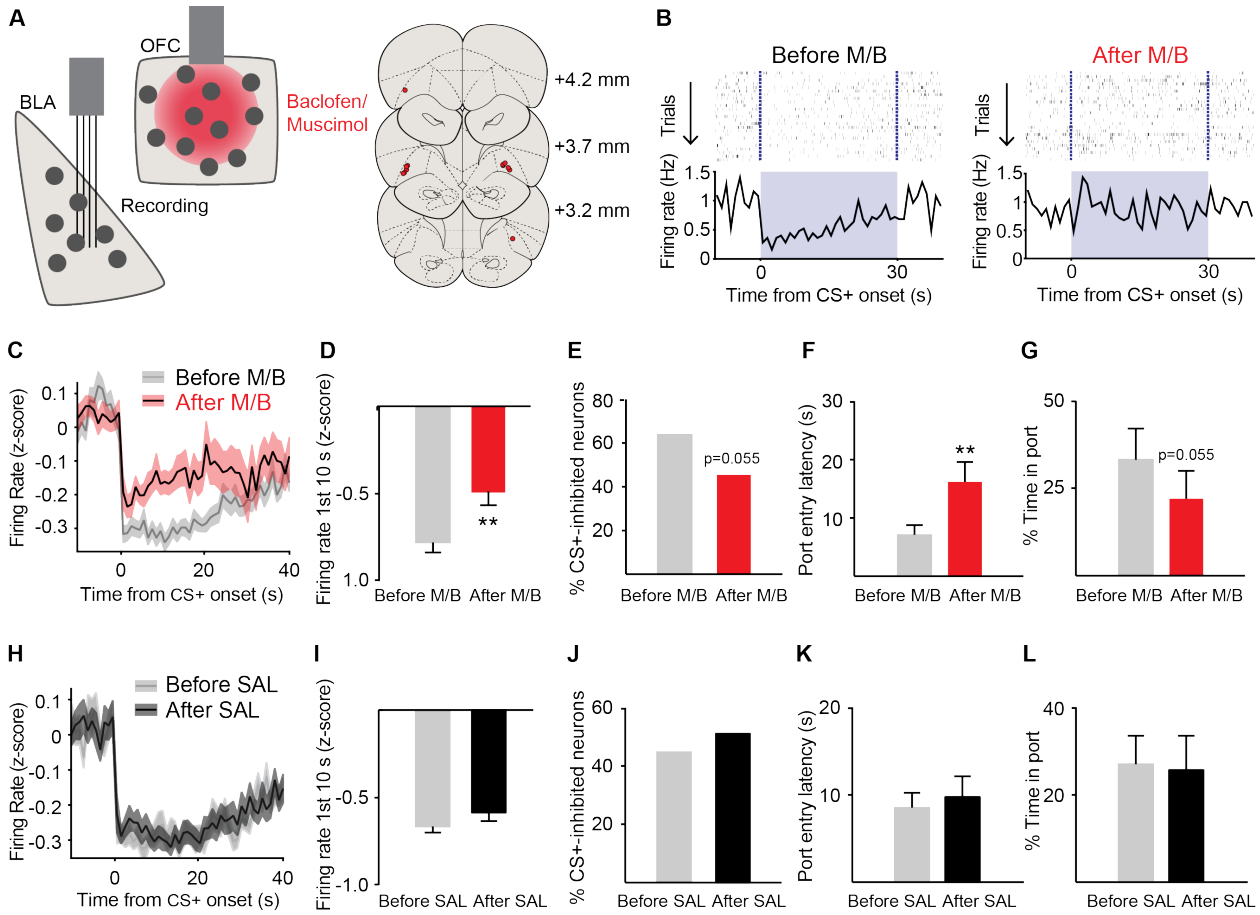

Figure 11: OFC activity is required for robust CS+-evoked inhibitions and conditioned behavior
(A) Left: experimental approach for OFC inactivation experiment. Rats were bilaterally implanted with electrode arrays in BLA and cannulae for drug infusion in OFC. In trained rats, BLA neurons were recorded in back-to-back conditioning sessions before and after OFC infusion with muscimol/baclofen (M/B) or saline. Right: cannula placements in OFC for rats used in the inactivation experiment (n=6).
(B) Peri-event rasters and histograms of a BLA neuron with a CS+-evoked sustained inhibition recorded before (left) and after (right) OFC inactivation with M/B.
(C) Population CS+-evoked response of all BLA neurons with sustained inhibitions recorded before and after OFC inactivation.
(D) Normalized firing rate in the first 10 s of the CS+ (mean ± SEM) of neurons with CS+-evoked inhibitions before M/B infusion into OFC, measured before and after the infusion. The firing rate in this period decreased after M/B (**P<0.01).
(E) Proportion of BLA neurons with CS+-evoked sustained inhibitions before and after OFC inactivation with M/B. This proportion decreased to a level that approached significance after M/B (P=0.055).
(F) Port entry latency after CS+ onset (mean ± SEM) in conditioning sessions before and after M/B infusion. This measure increased after M/B (P<0.01).
(G) Percent time in port during the first 10 s of the CS+ (mean ± SEM) in sessions before and after M/B. This measure decreased at a trend level after M/B (P=0.055).
(H-J) Data are presented as in C-G, but for the saline infusion. No measures were significantly different after compared to before saline infusion (all P>0.05).

Session	Baseline firing rate
Day 1	0.813 +/- 0.224
Day 7 (conditioning)	0.954 +/- 0.247
Day 8 (extinciton recall)	1.794 +/- 0.510 **
Before M/B	0.523 +/- 0.098
After M/B	0.578 +/- 0.115
Before saline	0.552 +/- 0.141
After saline	0.578 +/- 0.101

Table 1: Baseline firing rates of all recorded BLA neurons in various sessions
Firing rates are mean +/- sem. ** indicates a significant difference in baseline firing rate in the extinction recall session compared to the Day 7 conditioning session (*P*<0.01, Wilcoxon rank sum test). There was no significant difference in baseline firing rate for the following comparisons: Day 1 vs. Day 7, Before M/B vs. After M/B, or Before saline vs. After saline.

evoked response of neurons with sustained inhibitions during the CS^+ before OFC inactivation was reduced after M/B (p<0.01, Wilcoxon signed-rank test; Figures 11C and 11D). This decrease was also significant when only the first 500 ms after CS^+ onset was examined (p<0.01, Wilcoxon signed-rank test). The effect of M/B was not due to a change in baseline firing rates of BLA neurons after OFC inactivation (p=0.2057, Wilcoxon signed-rank test, Table S1). In addition, there was a trend toward a decrease in the number of neurons inhibited by the CS^+ from 63.6% (35/55) before inactivation to 45.5% (25/55) after inactivation (Figure 11E; χ^2=3.667, p=0.056). OFC inactivation also impaired the expression of conditioned port-entry behavior, as measured by an increase in port entry latency in response to the CS^+ (Figure 6F, p<0.004, paired sample t-test) while the decrease in percent time in port during the CS^+ did not attain significance (Figure 11G, p=0.055). None of these neural effects were observed after saline infusion into OFC (Figures 11H, 11I, and 11J), or for CS^+-excited neurons (Figure 12), and there was no change in behavioral responding after saline infusion into OFC (Figures 11K and 11L, paired sample t-

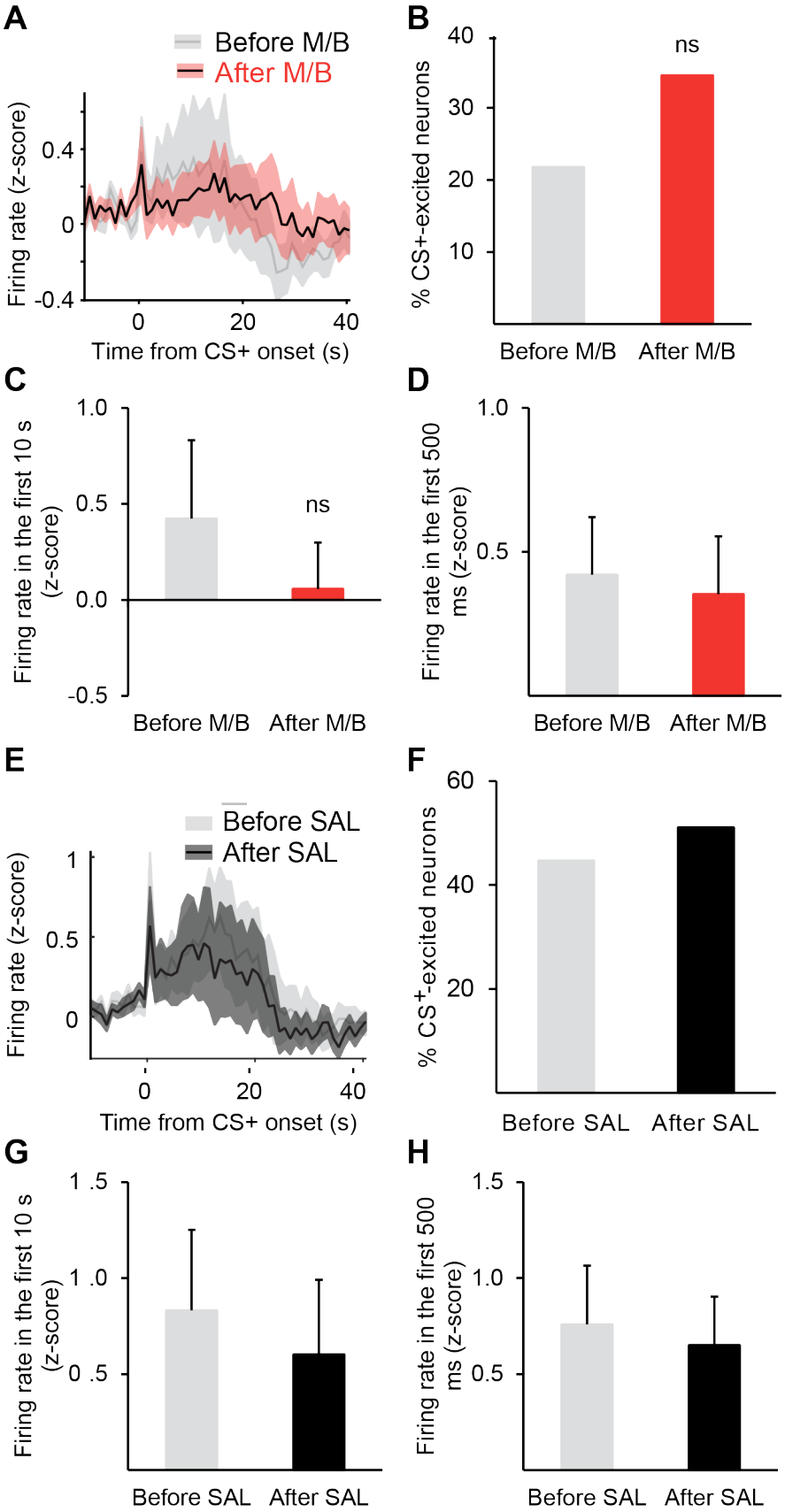
A
Before M/B
After M/B
Firing rate (z-score)
0.4
0
-0.4
0
20
40
Time from CS+ onset (s)
B
% CS+-excited neurons
40
30
20
10
ns
Before M/B
After M/B
C
Firing rate in the first 10 s (z-score)
1.0
0.5
0.0
-0.5
ns
Before M/B
After M/B
D
Firing rate in the first 500 ms (z-score)
1.0
0.5
Before M/B
After M/B
E
Before SAL
After SAL
Firing rate (z-score)
1
0.5
0
0
20
40
Time from CS+ onset (s)
F
% CS+-excited neurons
60
40
20
Before SAL
After SAL
G
Firing rate in the first 10 s (z-score)
1.5
1.0
0.5
Before SAL
After SAL
H
Firing rate in the first 500 ms (z-score)
1.5
1.0
0.5
Before SAL
After SAL

Figure 12: ***(continued from previous page)*** **Effect of OFC inactivation or saline infusion on CS+-excited BLA neurons**
(A) Population CS+-evoked response of all CS+-excited BLA neurons recorded before and after OFC inactivation.
(B) Proportion of CS+-excited BLA neurons before and after OFC inactivation. This proportion did not significantly change after M/B.
(C) Normalized firing rate in the first 10 s of the CS+ (mean ± SEM) of CS+-excited BLA neurons identified before OFC inactivation, measured before and after inactivation. There was no significant change in the normalized firing rate after inactivation.
(D) Normalized firing rate in the first 500 ms of the CS+ (mean ± SEM) of CS+-excited BLA neurons before and after OFC inactivation. There was no significant change in this measure after inactivation.
(E-H) Data are presented as in A-D, but for the saline infusion. No significant changes were observed after compared to before saline infusion into OFC (all P>0.05).

tests: port entry latency: p=0.220; time in port: p=0.603). These findings indicate that the OFC contributes to BLA inhibition as well as conditioned behavior elicited by the CS^+.

Optogenetic inhibition of the OFC-BLA projection during the CS^+ reduces conditioned behavioral responding

The OFC could impact BLA function via direct or indirect projections. To test the hypothesis that CS^+ conditioned responding depends upon a direct projection from OFC to BLA, we expressed the light-sensitive inhibitory opsin, ArchT3.0, in OFC neurons and placed optical fibers in the BLA to allow for selective inhibition of OFC inputs to BLA. Virus expression was robust in the OFC, primarily in the lateral compartment (Figures 13A and 13B). At the level of the BLA, robust terminal expression was seen in several regions (Figure 14A). OFC terminals clearly defined the BLA, but were mostly absent in the neighboring CeA (Figure 14B).

On test day, ArchT3.0-mediated inhibition of OFC terminals in the BLA (Figures 13C and 13D) during the CS^+ significantly reduced port entry time compared to CS^+ trials with no inhibition (p=0.0098; Figures 13E and 13F). For control rats expressing YFP-only virus, time in

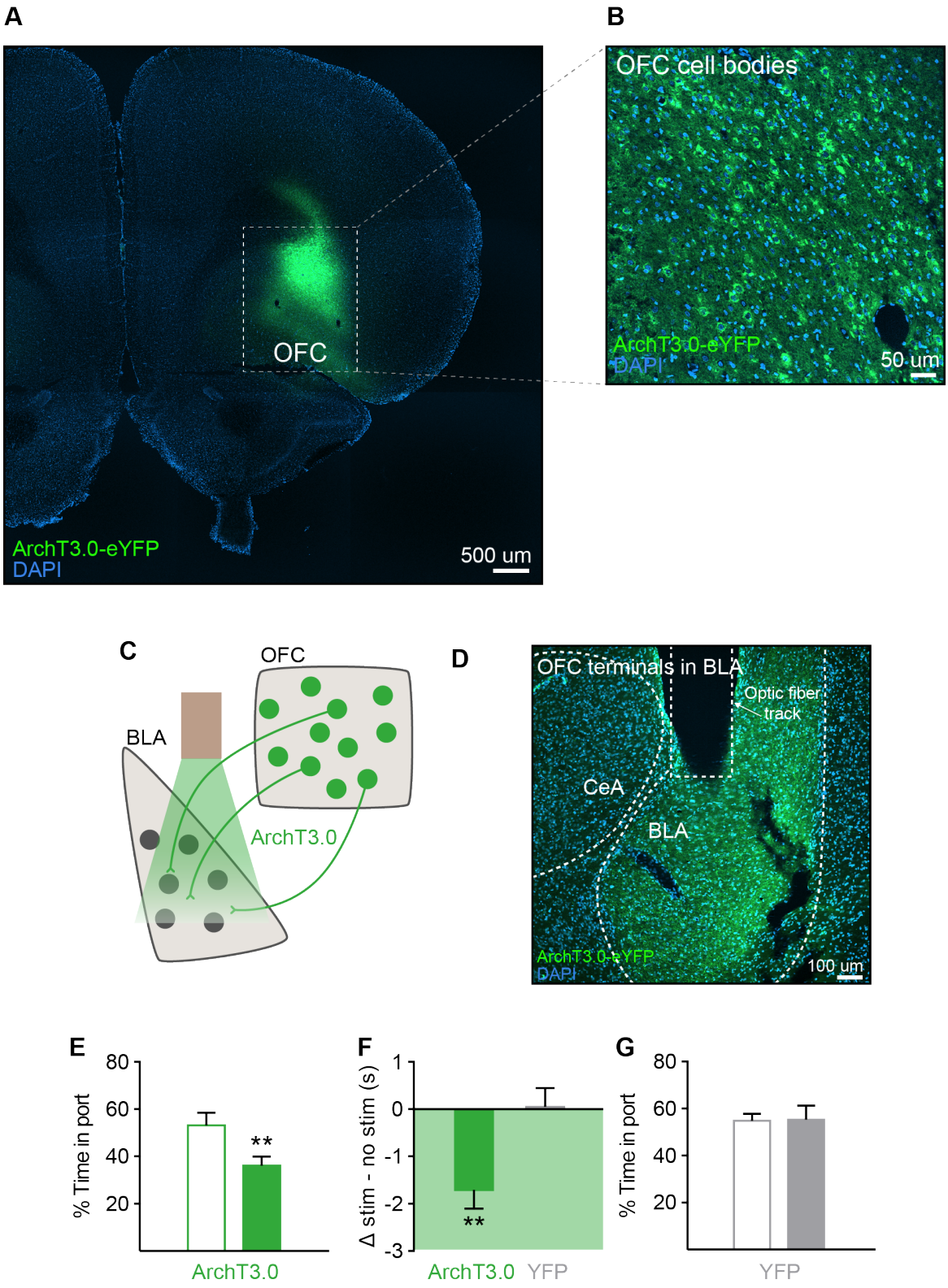
A
B
OFC cell bodies
OFC
ArchT3.0-eYFP
DAPI
500 um
ArchT3.0-eYFP
DAPI
50 um
C
OFC
BLA
ArchT3.0
D
OFC terminals in BLA
Optic fiber track
CeA
BLA
ArchT3.0-eYFP
DAPI
100 um
E
% Time in port
80
60
40
20
**
ArchT3.0
F
Δ stim - no stim (s)
1
0
-1
-2
-3
**
ArchT3.0
YFP
G
% Time in port
80
60
40
20
YFP

Figure 13: ***(continued from previous page)*** **Optogenetic inhibition of OFC-BLA terminals impairs conditioned behavior**
(A) Expression pattern following injection of AAV5-CaMKII-ArchT3.0-YFP into orbitofrontal cortex.
(B) OFC cell bodies expressing ArchT3.0-eYFP.
(C) Experimental approach for the OFC-to-BLA axon terminal inhibition experiment. Rats expressing AAV5-CaMKII-ArchT3.0-YFP (n=10) or AAV5-CaMKII-YFP (n=5) in OFC and implanted with a fiber optic in BLA were trained on the conditioning task described in Figure 1. On Day 8, half of CS+ and CS- trials were paired with light stimulation in BLA, serving to inhibit OFC-to-BLA axon terminals.
(D) Example histology for a rat used in the terminal inhibition experiment showing virus expression and fiber optic placement in BLA.
(E) Percent time in port during the first 10 s of the CS+ (mean ± SEM) during trials with light stimulation (solid) and during trials without stimulation (hollow). This measure significantly decreased in stimulated trials (**P<0.01).
(F) The difference in the percent time in port during the first 10 s of the CS+ (mean ± SEM) in trials with and without light stimulation for ArchT3.0-expressing rats (green), and YFP-only controls (grey). ArchT3.0-expressing rats, but not controls, demonstrated a change in percent time in port that was significantly different from zero.
(G) Percent time in port during the first 10 s of the CS+ (mean ± SEM) during trials with (solid) and without stimulation (hollow) for YFP-only control rats. There was no change in this measure in stimulation trials compared to no-stimulation trials (P=0.99).
(H-J) Data are presented as in E-G, but for port entry latency after the CS+. There was no significant change in latency between trials with and without stimulation for ArchT3.0-expressing rats or YFP-only rats (all P>0.05).

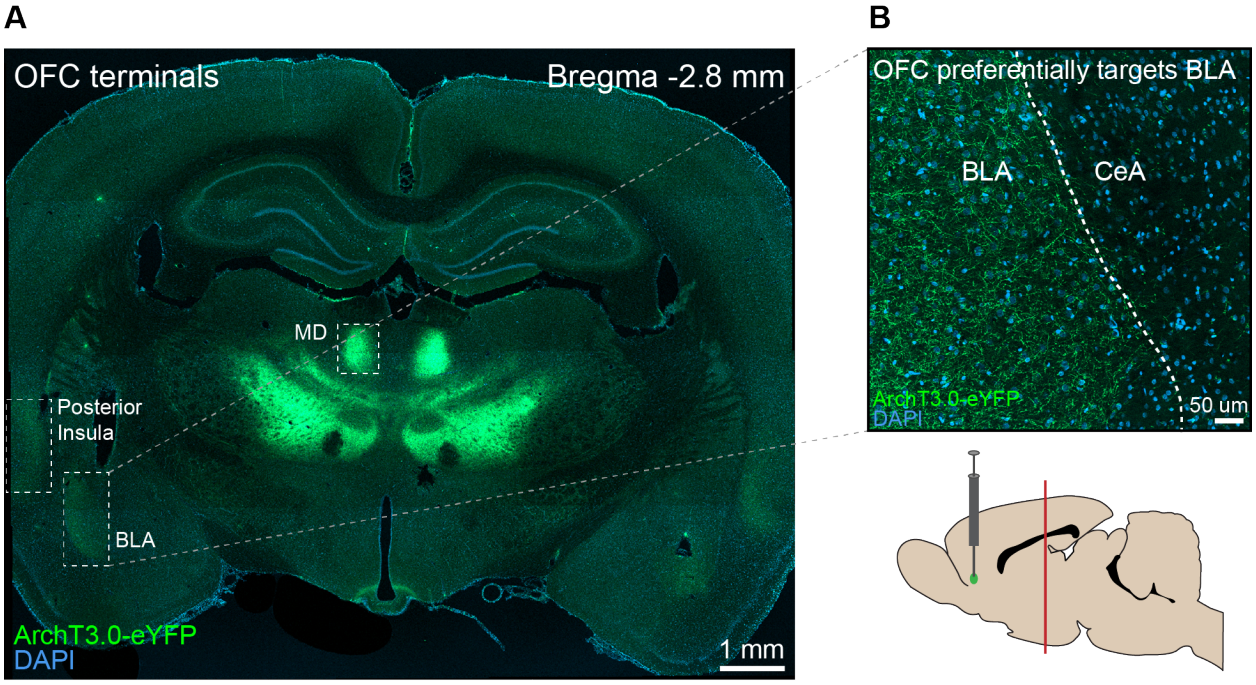

Figure 14: OFC viral expression and projections
(A) OFC terminals at the level of the BLA (-2.8mm from bregma), including mediodorsal (MD) thalamus, posterior insula, and BLA.
(B) OFC densely innervates BLA, but not CeA.

the port during the CS^+ was not affected by light delivery (p=0.99; Figure 13F and 13G). In contrast to the BLA stimulation experiment, port entry latency was not significantly altered (p=0.1816). Together, these findings suggest that a direct projection from OFC contributes to BLA neuron inhibition and conditioned behavior.

DISCUSSION

Here we reveal a new role for cue-evoked inhibition of BLA neurons in appetitive Pavlovian conditioned behavior. We found that inhibitory neural responses to the CS^+ emerged during acquisition and declined in extinction. In contrast, inhibition evoked by the CS^- diminished during acquisition, as rats learned to suppress behavioral responding to this cue. Thus, cue-evoked inhibition correlates with conditioned behavior across all stages of conditioning, consistent with the idea that this signal contributes to behavioral responding based on the learned significance of the cue. In support of this hypothesis, we found that optogenetic activation of BLA neurons during the CS^+ decreased conditioned responding to this cue. In addition, pharmacological inactivation of the OFC showed that OFC activity is required for robust cue-evoked inhibition in BLA, and may contribute to generation of this signal. In agreement with these findings, optogenetic inhibition of OFC terminals in the BLA reduced conditioned behavioral responding to the CS^+. Together, these results reveal a novel role for cue-evoked inhibition of BLA neurons in controlling conditioned responding to reward-predictive cues; further, these findings suggest that a neural circuit that includes projections from the OFC to the BLA is critical for both the cue-evoked BLA inhibition and cue-evoked conditioned responding.

Cue-evoked neuronal responses in the BLA

We found that neurons with sustained inhibitions during the CS^+ made up the large majority (77%) of recorded BLA units, consistent with our prior observations made in well-

trained subjects (Sangha et al., 2013; Shabel and Janak, 2009), Most other studies either do not report the proportion of neurons inhibited by cue presentation or report a smaller proportion. This may be in part because some statistical methods bias against detection of inhibitory responding. For example, studies that require a z- scored change in firing rate greater than +/- 2 in magnitude fail to detect sustained cue-evoked inhibitions in BLA neurons (Amano et al., 2011). This is likely because BLA neurons have variable and low baseline firing rates, such that a decrease from baseline to zero during the response period may not meet significance using this criterion. As another example, other studies focus on characterizing the differences in neural activity among multiple cues (Belova et al., 2008; Schoenbaum et al., 1998) (Belova et al., 2008; Schoenbaum et al., 1998), rather than explicitly differentiating between excitation and inhibition. These studies may have detected cue-evoked inhibitions without reporting them as such. In addition, some fear conditioning studies use a series of ~50 ms auditory pips as a conditioned stimulus in order to get more information from a single cue presentation. This approach requires averaging of the response to a single pip over a short (<100 ms) time bin, during which the long-lasting inhibitory response of the type examined here would likely be missed. In contrast, we used a long analysis window (10 s) to allow for characterization of the sustained inhibitions we observed, an approach that may facilitate detecting sustained inhibitory responses in low-firing neurons.

We detected a similar proportion of cue-excited neurons in trained animals as most previous studies have reported (≤25%) (Amano et al., 2011; Ambroggi et al., 2008; Herry et al., 2008; Roesch et al., 2010; Sangha et al.,2013). While we did not observe an increase in this proportion across training sessions, many of the neurons with cue-evoked excitation in the first training session rapidly lost this response as rats habituated to the cue. Thus, the neurons that

were cue-excited in session 7 likely gained this response during conditioning, consistent with previous reports and the established role of cue-excited neurons in promoting conditioned behavior (Ambroggi et al., 2008; Maren and Quirk, 2004; Quirk et al., 1995; Repa et al., 2001; Tye et al., 2008). However, we additionally found that in trained animals (session 7), 1/3 of cue-excited neurons (9/27) were putative inhibitory interneurons, a proportion that is greater than expected based on the estimates of interneuron frequency in the BLA (10-20%) (Woodruff and Sah, 2007, Pape and Pare, 2010). As we previously suggested (Shabel et al., 2011), this indicates that some of the population of cue-excited neurons commonly assumed to be projection neurons are actually interneurons.

It is not clear at the present time whether the nature of the conditioning procedure affects the relative proportions of excitatory and inhibitory neuronal responses. One way in which the present study differs from most others is the use of variable reward delivery latency. Arguing against the idea that this is a crucial element in promoting inhibitory cue encoding, previous studies from our laboratory using fixed reward delivery found that 40-50% neurons are inhibited by appetitive or aversive cues. Another possibility is that Pavlovian learning procedures lead to an increase in the relative proportion of inhibitory to excitatory cue-encoding neurons (e.g. Sangha et al., 2013; Shabel and Janak, 2009) compared to operant conditioning (e.g. Ambroggi et al., 2008; Tye et al., 2008). Future studies will be required to parametrically test these alternatives.

In summary, our findings confirm previous reports of the role of neuronal excitation, while also, together with previous reports, (Amano et al., 2011; Sangha et al., 2013; Shabel and Janak, 2009; Tye et al., 2008) highlighting the importance of considering cue-evoked inhibitions when defining BLA function.

Mechanism of cue-evoked inhibition in BLA

We found that activity of the OFC was required for robust cue-evoked inhibition in BLA as well as intact conditioned behavior. Optogenetic inhibition of OFC axon terminals in BLA also impaired conditioned port entry behavior, consistent with the hypothesis that this projection mediates cue-evoked inhibition in BLA, which in turn causally contributes to conditioned behavior. Based on evidence that OFC projections to BLA are glutamatergic (Aggleton et al., 1980; Amaral and Insausti, 1992), and on our findings that a cluster of putative interneurons in the BLA showed predominantly excitatory responding during the CS^+, we hypothesize that some OFC projections could provide feed-forward inhibition to BLA neurons by contacting local interneurons, as has been shown previously (Smith et al., 2000), or by contacting BLA projection neurons which in turn activate interneurons. Alternatively, it is also possible that OFC contributes to inhibition in BLA via activation of GABAergic cells in the intercalated cell masses (ITC). OFC projects directly to ITC cells (Ghashghaei and Barbas, 2002; Rempel-Clower, 2007; Smith et al., 2000), and both medial and lateral clusters of ITC cells project to and inhibit BLA projection neurons (Asede et al., 2015; Marowsky et al., 2005).

Recently, parvalbumin-expressing (PV+) interneurons in BLA were reported to exhibit enhanced firing during a conditioned fear cue, and PV+ interneuron photoactivation during the CS^+ was shown to increase fear-conditioned behavioral responses (Wolff et al., 2014). The authors showed that PV+ interneuron activation enhances or uncovers excitatory responses of a subset of putative projection neurons due to disinhibition via suppression of firing in somatostatin-expressing interneurons. In principle, interneurons that are cue-activated may also

inhibit projection neurons; in agreement, the same study showed that PV+ interneuron activation decreased spontaneous firing rates of putative projection neurons. The evidence presented here suggests that projection neuron inhibition may have also contributed to the observed increases in conditioned behavior.

Possible functions of cue-evoked inhibition in BLA

In what way could BLA neuron inhibition contribute to behavior? Given that our study involved conditioning to an appetitive cue, and that activation of the BLA can induce unconditioned fear behavior (Johansen et al., 2010; Tye et al., 2011), one superficially attractive possibility is that inhibition functions to suppress fear responding during conditioned reward-seeking. However, this hypothesis does not account for the findings that activation of discrete BLA neuron populations can mediate reward or fear (Namburi et al., 2015) and that BLA neurons can be inhibited by conditioned aversive stimuli in roughly equal proportions to appetitive stimuli (Sangha et al., 2013; Shabel and Janak, 2009). Indeed, the latter study used joint appetitive and aversive conditioning sessions and found that there was substantial overlap in neurons that were inhibited by appetitive and aversive cues. This observation suggests a possible alternative model: during conditioned behavior, the BLA neurons that are inhibited are those that promote responses other than the behavior of interest. This function is consistent with the sustained nature of cue-inhibitory signaling, that often mirrors the length of behavioral responding, as well as the finding that projection-specific optogenetic inhibition of BLA neurons facilitates cue-outcome learning (Namburi et al., 2015). In addition, because excitatory encoding of conditioned cues in the BLA is relatively sparse, i.e. <25% (Ambroggi et al., 2008; Herry et

al., 2008; Shabel and Janak, 2009), such a mechanism would allow enhancement of the signal-to-noise ratio of cue- excitatory signals. Given the role of OFC in decision making (Wallis, 2007) and encoding of anticipated outcomes (Schoenbaum et al., 1998, 2011), one function of the OFC-BLA projection could be to create or enhance inhibition of BLA neurons that do not promote behavioral responding in anticipation of that particular outcome, along with its demonstrated role in enhancing excitatory responses. The details of this interaction remain to be defined.

Roles of OFC and the OFC-to-BLA projection in task performance

As mentioned above, we found that OFC activity as well as OFC input to BLA is required for normal performance in our conditioning task. Multiple previous findings implicate the OFC in behavior mediated by Pavlovian conditioned cues (Burke et al., 2009; Ostlund and Balleine, 2007); however, this role is generally restricted to occasions in which a cue-evoked representation of the reward, and in particular, it's current value, is required for appropriate behavior (Holland and Gallagher, 2004; Pickens et al., 2003, 2005). It is not clear why cue-evoked behavioral responding was sensitive to OFC manipulations in the current study; however, we speculate that it may be due to the increased task demands induced by a reward delivery time that was unpredictable in the setting of a cue discrimination.

Interactions among the OFC and BLA in cue-dependent behavior have been demonstrated previously (Baxter et al., 2000; Churchwell et al., 2010; Izquierdo and Murray, 2004), although these studies cannot directly test for directionality. Examination of neural firing supports critical roles for both OFC-to-BLA projections and BLA-to-OFC projections (Morrison

et al., 2011; Saddoris et al., 2005; Schoenbaum et al., 2003). In primate, comparisons of local field potentials in OFC and BLA during reward-predictive cues find that OFC signals lead BLA signals in well-trained subjects (Morrison et al., 2011), suggesting an important role for the OFC-to-BLA projection. Here, by using projection-specific optogenetic approaches, we were able to isolate an effect on conditioned behavior of the OFC-to-BLA projection. Future studies targeting either the OFC-to-BLA projection or the reciprocal projection will be required to further understand their specific contributions to cue-driven behavior.

Conclusion

Reward-predictive cues produce both excitations and inhibitions in BLA neuronal populations. Here we show the inhibitions develop over learning and decrease during extinction, as shown previously for excitatory responses (Amano et al., 2011; Ambroggi et al., 2008; Quirk et al., 1995; Tye et al., 2008). Both conditioned behavior and the neuronal inhibitions in response to the cue are decreased when OFC input to the BLA is suppressed. Taken together, these findings emphasize a new role for inhibitory neural signals in the BLA in learned behavior in response to reward-predictive cues, and suggest a mechanism for this inhibition involving OFC input.

METHODS

Subjects

Adult male Sprague Dawley rats (Harlan, Indianapolis, IN) weighing ~250g-300g on arrival were singly housed under a 12 h light/dark cycle, lights on at 7:00 am. Rats had access to *ad libitum* food and water until 2 days prior to the onset of behavioral training and neural recording at which time they were restricted to 14.5-16.5g of food per day, maintaining ~90% of pre-restriction body weight. All procedures were approved by the Institutional Animal Care and Use Committees of UCSF, the Ernest Gallo Clinic and Research Center, and Johns Hopkins University, in accordance with guidelines of the US National Institutes of Health.

Surgery

For rats used in BLA neural recording experiments, standard stereotaxic surgical procedures were used to implant fixed microelectrode arrays (NeuroBiological Laboratories, Denison, TX) in the BLA (2.8 mm posterior to bregma; ±4.6 mm lateral to midline; 7.0 mm ventral to dura). Rats used for OFC inactivation experiments were implanted with 26-gauge stainless steel guide cannulae (Plastics One, Roanoke, VA) aimed at OFC (3.5 mm anterior to bregma; 2.8 mm lateral to midline; 2.7 mm ventral to skull) in addition to BLA electrode arrays. Guide cannulae were targeted 2 mm above the intended infusion site because infusion cannulae extended this distance beyond the end of the guide. For the BLA photoactivation experiment, rats were infused in the BLA bilaterally with adeno-associated viral vectors, AAV5-CaMKII-ChR2-YFP (ChR2; UNC Vector Core, Chapel Hill, NC) or AAV5-CaMKII-YFP (YFP; UNC Vector Core), to express channelrhodopsin-2 (ChR2)-YFP or YFP alone (0.5µl/side at 0.1µl/min; coordinates above); 300-µm optic fibers were additionally implanted 0.1 mm above the injection

sites. For the OFC axon terminal photoinhibition experiment, rats were infused bilaterally with AAV5-CaMKII-ArchT3.0-YFP (ArchT; UNC Vector Core) or the YFP control virus into the OFC (coordinates above), and implanted bilaterally with optic fibers above the BLA, as above.

Behavioral apparatus

Behavioral training and concomitant neural recording and optogenetic manipulation occurred in Plexiglas conditioning chambers (Med Associates, Georgia, VT) within sound-attenuating shells. A syringe pump located outside of each chamber within a Styrofoam box (to reduce sound emission) was used to deliver sucrose to a recessed port within one chamber wall. Entries into this port were tracked by an infrared beam traversing the port's threshold. Auditory stimuli were delivered through speakers located on the outside of the chamber walls, and a chamber light on the wall above the port provided constant illumination. MedPC (Med Associates) software controlled the behavioral programs and recorded behavioral data.

Neural recording in the BLA during Pavlovian conditioning

Three days before the start of behavioral training, rats (n=18) were pre-exposed to sucrose in the home cage for 48 hours. Rats were then trained on an appetitive Pavlovian conditioning task for ~2 hrs/day for 7 days. Conditioning consisted of 30 presentations each of two auditory stimuli, a 2.9 kHz tone or white noise, delivered for 30s, at ~70dB, 2 min variable ITI, with one stimulus paired with delivery of 0.2ml of a 10% sucrose solution over 6 s. Choice of stimulus paired with sucrose reward was counterbalanced across animals. Sucrose delivery during the cue was variable, usually occurring between 10-24 s after cue onset, but occurring

after 1 s on ~6% of trials. Sucrose delivery latency was variable to discourage conditioned responding based on timing and to encourage conditioned responding throughout the cue period.

Extinction training and testing

Fourteen of 18 rats trained on Pavlovian conditioning underwent behavioral extinction. Within-session extinction training was conducted Day 7 of conditioning: the 7th conditioning session was modified to include 60 presentations each of the CS^+ and CS^-, and after the first 30 CS^+ presentations, the pump drive was manually retracted from the end of the syringe containing sucrose, such that the last 30 CS^+ presentations were unreinforced. Within-session extinction was conducted to allow reliable identification of units across both training and extinction. On the following day, animals underwent a second extinction session consisting of 30 unreinforced presentations of both the CS^+ and CS^- to test for extinction learning recall.

Pharmacological inactivation of OFC

Six rats with guide cannulae implanted in OFC and microelectrode arrays implanted in BLA underwent 5 days of training on the appetitive task described above. For the next 6 days, rats were trained on a modification consisting of two 1-hour sessions with 15 presentations each of the CS^+ and CS^-, separated by either an intracranial sham infusion, saline infusion or drug infusion. The schedule of infusions was as follows: Days 6, 8, and 10, sham infusions; Day 7, saline infusion; Days 9 and 11, drug infusion or saline infusion. Only infusions on Days 9 and 11 were used for experimental analysis (the remainder were for habituation), with the order of treatment on Days 9 and 11 counterbalanced. Rats received 0.5 μl infusions (0.3 μl/min) of a cocktail (M/B) of the $GABA_A$ agonist muscimol (250ng/μl) and the $GABA_B$ agonist baclofen

(250ng/μl) or saline as described (Chaudhri et al., 2010). Infusion cannulae were left in place for 2 min after infusion to allow for diffusion, and subjects returned to the conditioning chamber after ~8 min.

Optogenetic activation of BLA

Rats infused with an AAV5-CaMKII-ChR2-YFP (n=9) or AAV5-CaMKII-YFP (n=6) and fiber optic implants in the BLA received the 7-day appetitive training as described above. During this period, rats were tethered with an optic cable to a liquid swivel rotary joint, which was connected to a 100mW 473nm blue DPSS laser (OEM Laser Systems, Midvale, UT), but no light was delivered. On day 8, light (5-ms pulses, 20 Hz) was delivered during the first 10 s of 50% of CS^+ and 50% of CS^- trials. Sucrose was available as usual.

Optogenetic inhibition of OFC terminals in BLA

Rats infused with AAV5-CaMKII-ArchT3.0-YFP (n=10) or AAV5-CaMKII-YFP (n=5) in OFC and fiber optic implants in the BLA were tethered to a 532nm green DPSS laser and trained as in the BLA optogenetic activation study. On the test day, light (10-s constant pulse) was delivered during the first 10 s of 50% of CS^+ and 50% of CS^- trials, and sucrose was available as usual.

Histology

Brains were fixed via transcardial perfusion. For electrophysiology studies, formalin solution containing 3% potassium ferrocyanide was used during perfusion and as a post-fixative agent to allow for later visualization of electrode tips in 50 μm Nissl-stained coronal sections.

Only neurons recorded on electrodes confirmed to be within the LA or BA were included in the analysis. For optogenetic studies, rats were perfused with 4% paraformaldehyde. For initial viral expression and placement verification sections were coverslipped with Vectashield containing DAPI and imaged for YFP fluorescence and verification of optic fiber placements above the BLA. Sections were imaged using a Zeiss Axio Imager 2 microscope.

Immunohistochemistry

Immunohistochemistry was as described before (Witten et al, 2011). Fifty μm sections were incubated in bovine serum albumin (BSA) and Triton X-100 (each 0.2%) for 20 min, followed by 10% normal donkey serum (NDS) for 30 min. Sections were incubated in mouse anti-GFP antibody (1:1500, Invitrogen) overnight at 4°C. Sections were then washed and incubated for 10 min with 2% NDS in PBS; secondary antibody conjugated to Alexa Fluor 488 (Invitrogen) was added (1:200) for 2 hours. Finally, sections were washed, mounted, air-dried, and coverslipped with Vectashield containing DAPI for imaging.

Single-unit recording and discrimination

Neuronal activity was recorded with commercial hardware and software (Plexon, Dallas, TX), and single units were identified offline (Plexon). Principal component analysis (PCA) was performed on unsorted waveforms based on their shape, and PCA scores were plotted in two- or three-dimensional space. In this space, clusters of waveforms with similar PCA scores were defined manually, and were considered to correspond to a valid single unit if 1) the cluster was physically separate from clusters corresponding to other units, 2) waveforms within the cluster

had a visually similar shape, and 3) spikes from the cluster displayed a clear refractory period of at least 1 ms.

Classification and analysis of CS responses

Recording files with single-unit clusters defined were imported into NeuroExplorer (Plexon) software to create peri-stimulus time histograms (PSTHs) aligned to onset of the CS^+ and CS^- for each defined unit. Neural timestamps imported from NeuralExplorer to Matlab (Mathworks, Natick, MA) were analyzed as follows. To determine whether individual neurons exhibited a significant response at the onset of a cue ("early response"), the mean firing rate during each of five 50-ms bins during a 250-ms response window after cue onset on each trial was compared to the mean firing rate in 50-ms bins during a 10-s baseline period beginning 20 s prior to cue onset using a Wilcoxon signed rank test. If the firing rate was significantly different from baseline ($p<0.01$) during at least one of the 50-ms bins in the response window, the early response was deemed significant. Significant "sustained responses" were detected in the same way except the size of the baseline bin and response bin were both 10 s, and the baseline window started 10 s before cue onset. For CS^+ measures, trials with 1-s reward delivery latencies were excluded from both of these analyses. For each type of response (early or sustained), if the firing rate in the response window was significantly higher than baseline, the response was classified as excitatory, and if it was significantly lower, the response was classified as inhibitory. In this study, we focused on neurons with sustained inhibitory responses, as fewer than 2% of the neural population on any given session demonstrated early inhibitory responses in the absence of sustained inhibitions during the CS^+. Neurons with either an early or sustained CS-evoked excitation were classified as CS-excited. Neurons that possessed both an excitatory early

response and an inhibitory sustained response (0-10.5% of the total neural population on any given session) were classified as CS-excited as well as having a sustained inhibition for most analyses. However, these neurons were classified as multiphasic when comparing the distribution of CS^+-evoked responses in putative interneurons and putative projection neurons on Day 7. Only one neuron had an inhibitory early response and excitatory sustained response to the CS^+ on any of the recording sessions, and this occurred on Day 1. This neuron was counted as a CS^+-excited neuron on this day. Finally, neurons were classified as not cue-responsive if they had no significant early or sustained cue response.

We also obtained normalized early and sustained cue responses by calculating z-scores of the change in firing rate from baseline during a set response window after CS^+ onset: 500 ms for the early response and 10 s for the sustained response. Z-score calculations also used different measures of baseline firing rate: the firing rate in 500 ms bins during a 10 s baseline window prior to CS^+ onset for the early response, and the firing rate during the entire 10 s baseline window for the sustained response. This resulted in a consistent difference in the magnitude of the z-score for the sustained response and the early response.

To be classified as increasing inhibitory response in the first session, neurons had to display a significant negative correlation between normalized firing rate in the 10-s period after cue onset and trial number, and possess a negative mean z-score in this period across trials. The converse criteria were used for classification as decreasing inhibitory responding in the first session. Neurons that increased excitatory responding to the CS^+ in the first training session were classified as those that had a positive correlation between firing rate in either the first 500 ms or the first 10s after cue onset and had a mean positive z-scored firing rate in the relevant period, and the converse criteria were used for classification as losing an excitatory response.

We used the Wilcoxon rank sum test to compare baseline firing rates of CS^+-inhibited neurons between sessions.

Analysis of the effects of OFC inactivation

For both saline and M/B infusions into the OFC, neurons with CS^+-evoked sustained inhibitions were identified in the pre-infusion session, and the normalized CS^+ responses and baseline firing rates were compared before and after infusion using the Wilcoxon signed-rank test. We also compared the number of neurons with sustained inhibitions before and after saline or M/B infusions using the chi-squared test.

Identification of putative BLA interneurons

Putative interneurons in BLA were identified by cluster analysis of spiking characteristics of all BLA neurons recorded during the final conditioning session on Day 7. The spiking characteristics used were area under the afterhyperpolarization peak (AUP), log of baseline firing rate, and spike half width (measured as the distance between action potential peak and trough). Initially, k-means clustering was employed to identify two statistically separate clusters and then a more restricted cluster of putative interneurons was manually defined based on visual cluster separation. Neurons with values within the following bounds were included in this latter cluster: AUP>25μV*s, log of baseline firing rate >0.2, and spike half width <300ms. Classification of putative INs' and undefined BLA neurons' CS^+ response type was performed as described above (*Classification and analysis of CS responses*). The baseline firing rate of all BLA neurons recorded in the conditioning session on Day 7 was correlated with their normalized early and sustained responses to the CS^+ using linear regression.

Behavioral measures and analysis

The percentage of time rats spent in the sucrose port during each CS presentation was calculated by dividing the amount of time the rat's nose was in the port during the first 10 s of the CS by the total time (10 s) and multiplying by 100%. Port entry latency on each trial was calculated by subtracting the time of CS onset from the time at which the rat first entered the port after CS onset. Trial latency was set to 30 s if the subject did not enter the port during the CS. Trials in which the reward was delivered 1s after CS^+ onset (~6%) were excluded from analysis.

The change in time spent in port and port entry latency for CS^+ and CS^- across conditioning sessions 1-7 were assessed by two-way repeated measures ANOVA analyses with training session and cue type as within-subjects factors, as well as one-way repeated measures ANOVAs for each cue, with Greenhouse-Geisser correction used when indicated. Wilcoxon-signed rank tests were used to determine whether CS^+ measures of time in port and port entry latency changed between behavioral sessions.

After OFC pharmacological inactivation, Wilcoxon signed-rank tests were used to compare time spent in port during the CS^+ and port entry latency after CS^+ onset before and after each infusion.

For optogenetic manipulations, time spent in the sucrose port during the first 10 s of cue presentations and the latency to first port entry after cue onset were compared for trials with laser stimulation versus trials without stimulation with Wilcoxon signed-rank tests. The degree of change in port entry time and latency was analyzed with one-sample Wilcoxon signed-rank tests.

Neural correlations with behavior

To test whether more BLA neurons were CS^+-inhibited in rats that demonstrated rapid acquisition of conditioning in the first session, the mean port entry latency and the proportion of BLA neurons inhibited by the CS^+ were calculated for each rat with detectable BLA units on Day 1 (N=16) and a linear regression analysis was performed to compare the two sets of values.

We used chi-square tests to determine if there was a change in the number of neurons showing either excitatory or inhibitory responses between different behavioral sessions.

REFERENCES

Aggleton, J.P., Burton, M.J., and Passingham, R.E. (1980). Cortical and subcortical afferents to the amygdala of the rhesus monkey (Macaca mulatta). Brain Res. *190*, 347–368.

Amano, T., Duvarci, S., Popa, D., and Pare, D. (2011). The Fear Circuit Revisited: Contributions of the Basal Amygdala Nuclei to Conditioned Fear. J. Neurosci. *31*, 15481–15489.

Amaral, D.G., and Insausti, R. (1992). Experimental Brain Research. *88*, 375–388.

Ambroggi, F., Ishikawa, A., Fields, H.L., and Nicola, S.M. (2008). Basolateral Amygdala Neurons Facilitate Reward-Seeking Behavior by Exciting Nucleus Accumbens Neurons. Neuron *59*, 648–661.

Baxter, M.G., Parker, a, Lindner, C.C., Izquierdo, a D., and Murray, E. a (2000). Control of response selection by reinforcer value requires interaction of amygdala and orbital prefrontal cortex. J. Neurosci. *20*, 4311–4319.

Belova, M.A., Paton, J.J., Morrison, S.E., and Salzman, C.D. (2007). Expectation modulates neural responses to pleasant and aversive stimuli in primate amygdala. Neuron. *55*, 970-984.

Belova, M.A., Paton, J.J., and Salzman, C.D. (2008). Moment-to-moment tracking of state value in the amygdala. J. Neurosci. *28*, 10023–10030.

Burke, K. a., Takahashi, Y.K., Correll, J., Leon Brown, P., and Schoenbaum, G. (2009). Orbitofrontal inactivation impairs reversal of Pavlovian learning by interfering with "disinhibition" of responding for previously unrewarded cues. Eur. J. Neurosci. *30*, 1941–1946.

Capogna, M. (2014). GABAergic cell type diversity in the basolateral amygdala. Curr. Opin. Neurobiol. *26*, 110–116.

Churchwell, J.C., Morris, A.M., Heurtelou, N.M., and Kesner, R.P. (2009). *Behav. Neurosci*. *123*, 1185–1196.

Courtin, J., Chaudun, F., Rozeske, R.R., Karalis, N., Gonzalez-Campo, C., Wurtz, H., Abdi, A., Baufreton, J., Bienvenu, T.C.M., and Herry, C. (2014). Prefrontal parvalbumin interneurons shape neuronal activity to drive fear expression. Nature *505*, 92–96.

Herry, C., Ciocchi, S., Senn, V., Demmou, L., Müller, C., and Lüthi, A. (2008). Switching on and off fear by distinct neuronal circuits. Nature *454*, 600–606.

Holland, P.C., and Gallagher, M. (2004). Amygdala-frontal interactions and reward expectancy. Curr. Opin. Neurobiol. *14*, 148–155.

Izquierdo, A., and Murray, E. a (2004). Combined unilateral lesions of the amygdala and orbital prefrontal cortex impair affective processing in rhesus monkeys. J. Neurophysiol. *91*, 2023–2039.

Janak, P., and Tye, K. (2015). From circuits to behaviour in the amygdala. Nature. *517*, 284-29

Johansen, J.P., Hamanaka, H., Monfils, M.H., Behnia, R., Deisseroth, K., Blair, H.T., and LeDoux, J.E. (2010). Optical activation of lateral amygdala pyramidal cells instructss associative fear learning. PNAS. *107*, 12692-12697.

LeDoux, J.E., Cicchetti, P., Xagoraris, a, and Romanski, L.M. (1990). The lateral amygdaloid nucleus: sensory interface of the amygdala in fear conditioning. J. Neurosci. *10*, 1062–1069.

Maren, S., and Quirk, G.J. (2004). Neuronal signalling of fear memory. Nat. Rev. Neurosci. *5*, 844–852.

McKernan, M.G., and Shinnick-Gallagher, P. (1997). Fear conditioning induces a lasting potentiation of synaptic currents in vitro. Nature *390*, 607–611.

Morrison, S.E., Saez, A., Lau, B., and Salzman, C.D. (2011). Different Time Courses for Learning-Related Changes in Amygdala and Orbitofrontal Cortex. Neuron *71*, 1127–1140.

Muramoto, K., Ono, T., Nishijo, H., and Fukuda, M. (1993). Rat amygdaloid neuron responses during auditory discrimination. Neuroscience *52*, 621–636.

Ostlund, S.B., and Balleine, B.W. (2007). Orbitofrontal cortex mediates outcome encoding in Pavlovian but not instrumental conditioning. J. Neurosci. *27*, 4819–4825.

Pape, H.C. and Pare, D. (2010). Plastic synaptic networks of the amygdala for the acquisition, expression, and extinciton of conditioned fear. Physiol. Rev. *90*, 419-463.

Paton, J.J., Belova, M. a, Morrison, S.E., and Salzman, C.D. (2006). The primate amygdala represents the positive and negative value of visual stimuli during learning. Nature *439*, 865–870.

Pickens, C.L., Saddoris, M.P., Setlow, B., Gallagher, M., Holland, P.C., and Schoenbaum, G. (2003). Different roles for orbitofrontal cortex and basolateral amygdala in a reinforcer devaluation task. J. Neurosci. *23*, 11078–11084.

Pickens, C.L., Saddoris, M.P., Gallagher, M., and Holland, P.C. (2005). Devaluation Task. *119*, 317–322.

Quirk, G.J., Repa, C., and LeDoux, J.E. (1995). Fear conditioning enhances short-latency auditory responses of lateral amygdala neurons: parallel recordings in the freely behaving rat. Neuron *15*, 1029–1039.

Repa, J.C., Muller, J., Apergis, J., Desrochers, T.M., Zhou, Y., and LeDoux, J.E. (2001). Two different lateral amygdala cell populations contribute to the initiation and storage of memory. Nat. Neurosci. *4*, 724–731.

Roesch, M.R., Calu, D.J., Esber, G.R., and Schoenbaum, G. (2010). Neural correlates of variations in event processing during learning in basolateral amygdala. J. Neurosci. *30*, 2464–2471.

Saddoris, M.P., Gallagher, M., and Schoenbaum, G. (2005). Rapid associative encoding in basolateral amygdala depends on connections with orbitofrontal cortex. Neuron *46*, 321–331.

Sanders, S.K., and Shekhar, a (1991). Blockade of GABAA receptors in the region of the anterior basolateral amygdala of rats elicits increases in heart rate and blood pressure. Brain Res. *567*, 101–110.

Sangha, S., Chadick, J.Z., and Janak, P.H. (2013). Safety encoding in the basal amygdala. J. Neurosci. *33*, 3744–3751.

Schoenbaum, G., Chiba, A.A., and Gallagher, M. (1998). Orbit ofront al cort ex and basolat eral am ygdala encode expect ed out com es during learning. 155–159.

Schoenbaum, G., Chiba, a a, and Gallagher, M. (1999). Neural encoding in orbitofrontal cortex and basolateral amygdala during olfactory discrimination learning. J. Neurosci. *19*, 1876–1884.

Schoenbaum, G., Setlow, B., Saddoris, M.P., and Gallagher, M. (2003). Encoding predicted outcome and acquired value in orbitofrontal cortex during cue sampling depends upon input from basolateral amygdala. Neuron *39*, 855–867.

Schoenbaum, G., Roesch, M.R., Stalnaker, T. a, and Takahashi, Y.K. (2011). Orbitofrontal Cortex and Outcome Expectancies: Optimizing Behavior and Sensory Perception. Neurobiol. Sensat. Reward 1–17.

Shabel, S.J., and Janak, P.H. (2009). Substantial similarity in amygdala neuronal activity during conditioned appetitive and aversive emotional arousal. Proc. Natl. Acad. Sci. U. S. A. *106*, 15031–15036.

Smith, Y., Paré, J.F., and Paré, D. (2000). Differential innervation of Parvalbumin-immunoreactive interneurons of the basolateral amygdaloid complex by cortical and intrinsic inputs. J. Comp. Neurol. *416*, 496–508.

Tye, K.M., and Janak, P.H. (2007). Amygdala neurons differentially encode motivation and reinforcement. J. Neurosci. *27*, 3937–3945.

Tye, K.M., Stuber, G.D., de Ridder, B., Bonci, A., and Janak, P.H. (2008). Rapid strengthening of thalamo-amygdala synapses mediates cue-reward learning. Nature *453*, 1253–1257.

Tye, K.M., Prakash, R., Kim, S.-Y., Fenno, L.E., Grosenick, L., Zarabi, H., Thompson, K.R., Gradinaru, V., Ramakrishnan, C., and Deisseroth, K. (2011). Amygdala circuitry mediating reversible and bidirectional control of anxiety. Nature *471*, 358–362.

Wallis, J.D. (2007). Orbitofrontal cortex and its contribution to decision-making. Annu. Rev. Neurosci. *30*, 31–56.

Wolff, S.B.E., Gründemann, J., Tovote, P., Krabbe, S., Jacobson, G. a, Müller, C., Herry, C., Ehrlich, I., Friedrich, R.W., Letzkus, J.J., et al. (2014). Amygdala interneuron subtypes control fear learning through disinhibition. Nature *509*, 453–458.

Woodruff, A.R., and Sah, P. (2007). Networks of parvalbumin-positive interneurons in the basolateral amygdala. J. Neurosci. *27*, 553–563.

Publishing Agreement

It is the policy of the University to encourage the distribution of all theses, dissertations, and manuscripts. Copies of all UCSF theses, dissertations, and manuscripts will be routed to the library via the Graduate Division. The library will make all theses, dissertations, and manuscripts accessible to the public and will preserve these to the best of their abilities, in perpetuity.

Please sign the following statement:

I hereby grant permission to the Graduate Division of the University of California, San Francisco to release copies of my thesis, dissertation, or manuscript to the Campus Library to provide access and preservation, in whole or in part, in perpetuity.

Kate Mtale

Author Signature

Sept 9, 2015

Date